THE STRUCTURAL GEOLOGY OF THE WESTERN MARGIN OF THE ENTIA DOME, HARTS RANGE, EASTERN ARUNTA INLIER.

by

PRU J. MACDONALD

November, 1986

(1)

The Structural Geology of the Western Margin of the Entia Dome, Harts Range, Eastern Arunta Inlier

Pru J. Macdonald

Thesis submitted as partial fulfilment for the Honours Degree of Bachelor of Science.

November 1986

Department of Geology and Geophysics
The University of Adelaide

National Grid Reference SF–53 5951 (1:100 000)

Abstract

The study area is located within the eastern Harts Ranges, approximately 150 km ENE of Alice Springs in the Proterozoic Arunta Inlier, central Australia. Detailed geological mapping at a scale of 1:12 500 has included lithologies of the Entia gneiss complex within the Entia Dome, the Irindina supracrustal assemblage and the Bruna gneiss (terminology after Ding and James, 1985).

The 'basement' lithologies of the Entia gneiss complex have undergone at least three repeated, generally isoclinal, recumbent folding events and peak (upper amphibolite facies) metamorphism prior to intrusion of the Bruna gneiss. The metapelitic lithologies of the Irindina supracrustal assemblage ('cover') have been subject to at least one isoclinal folding event prior to its juxtaposition with the 'basement'.

Emphasis is on the Bruna gneiss, interpreted as a variably mylonitised orthogneiss that was emplaced along a wide ductile shear zone that separated the 'cover' and 'basement'. This study subdivides the Bruna gneiss into two lithologies on the basis of field and microstructural observations and strain analysis: the structurally lower Granitic gneiss and the overlying (much thinner) Megacrystic gneiss. The Megacrystic gneiss, previously described as mylonite derived from the Granitic gneiss, is interpreted as having been intruded independantly from the bulk of the Bruna (*ie* Granitic) gneiss, and has undergone less complex deformation relative to the Granitic gneiss.

Contents

Chapter 1: Introduction 1

1.1 Location of the study area 1
1.2 Previous Investigations 1
1.3 Aims of this project 2
1.4 Methods 2

Chapter 2: Description of Lithologies 3

2.1 Introduction 3
2.2 Lithologies of the Entia gneiss complex 3
2.2.1 Quartzofeldspathic gneiss 3
2.2.2 Kyanite-biotite schist 4
2.2.3 Layered amphibolites 4
2.2.4 Calc-silicates 5
2.2.5 Massive amphibolite 6
2.2.6 Felsic gneiss 6
2.2.7 Minor quartzites, schists and augen gneisses 6
2.2.8 Meta-ultramafic 7
2.2.9 Origin of the Entia gneiss complex lithologies 8
2.3 Bruna gneiss 8
2.3.1 Granitic gneiss 9
2.3.2 Megacrystic gneiss 10
2.4 Irindina supracrustal assemblage 10
2.4.1 Amphibolite 10
2.4.2 Biotite-garnet schists 11
2.4.3 Impure marble 11
2.4.4 Felsic megacrystic and mylonitic gneisses 11
2.5 Metamorphic Conditions 12

Chapter 3: Structural Relationships 13

3.1 Introduction 13
3.2 Methods and Terminology 13
3.3 Structures of the Entia gneiss complex 13
3.3.1 First Deformation ED_1 13
3.3.2 Second Deformation ED_2 14
3.3.3 Third Deformation ED_3 14
3.3.4 Fourth Deformation ED_4 15
3.3.5 Fifth and Subsequent Deformations 15

3.4 Structures of the Bruna gneiss 15
3.4.1 First Deformation BD_1 15
3.4.2 Second Deformation BD_2 16
3.4.3 Third Deformation BD_3 16
3.4.4 Fourth Deformation BD_4 16
3.4.5 Fifth Deformation BD_5 17
3.5 Structures of the Irindina supracrustal assemblage 17
3.5.1 First Deformation ID_1 17
3.5.2 Second Deformation ID_2 17
3.5.3 Third Deformation ID_3 17
3.6 Structural Summary 18

Chapter 4: Microfabrics 19
4.1 Introduction 19
4.2 Microstructures of the Entia gneiss lithologies 19
4.3 Microstructures of ED_2 19
4.4 Microstructures of Post-ED_2 Deformations 20
4.5 Microstructures of the Bruna gneiss 21
4.6 Microstructures Associated with BD_1 22
4.7 Microstructures of Post BD_1 Deformations 23
4.8 Microstructures of the Irindina supracrustal assemblage 24

Chapter 5: Strain and Kinematic Analysis 26
5.1 Introduction 26
5.2 Movement Direction 26
5.3 Sense of Shear 26
5.4 Strain Analysis 27
5.5 Discussion 28

Chapter 6: Discussion and Tectonic Synthesis 29

Acknowledgements 31

References 32

Appendix I: Thin Section Descriptions 37

Appendix II: Thin Section Preparation 45

Appendix III: Strain Analysis and Methods 46

List of Figures

Figure 1.1: Geological and tectonic map of the Harts Range area.
Figure 3.1: Summary of the major structural elements of the map area.
Figure 3.2: Stereographic projections.
Figure 3.3: Field sketches.
Figure 3.4: 'Anatomy' of BF_3 (steep zones).
Figure 3.5: Maps of lineation trends and contoured foliation dips.
Figure 5.1: Cartoon of asymmetric augen.
Figure 5.2: Flinn plots.
Figure 6.1: Tectonic evolution of the Harts Range area.
Figure 6.2: Structural development of the Bruna gneiss.

List of Tables

Table I: Structural summary.
Table II: Data from shear sense analysis.

List of Plates

Plate 1: Representative outcrop of the Layered amphibolite map unit.
Plate 2: Representative outcrop of the Grey gneiss map unit.
Plate 3: Migmatite.
Plate 4: Lineated felsic gneiss.
Plate 5: Cleavage development in EF_3 folds.
Plate 6: Calc-silicate boudins within the impure marble.
Plate 7: Layered amphibolite lens.
Plate 8: Granitic gneiss lineation plunging west.
Plate 9: Layered amphibolite with EF_1 folds.
Plate 10: Granitic gneiss with recumbent BF_2 folds.
Plate 11: Migmatitic banding within the Grey gneiss map unit.
Plate 12: Buckling of the EF_4 fold hinge.
Plate 13: Asymmetric EF_4 closure, refolding EF_3 hinge.
Plate 14: Calc-silicate rotated boudins within EF_4 fold closure.
Plate 15: Disharmonic folding associated with EF_3.
Plate 16: Asymmetric EF_4 fold closure in Layered amphibolite map unit.
Plate 17: Warping of recumbant EF_2 folds by ED_5 deformation.
Plate 18: Isoclinal recumbant BF_1 folds in Granitic gneiss.
Plate 19: Ptygmatic BF_2 folds in Granitic gneiss.
Plate 20: Granitic gneiss folded by BF_3 folds (steep zone).
Plate 21: Isoclinal BF_2 folding contact between Granitic and Megacrystic gneisses.
Plate 22: Lineation in XY section of Megacrystic gneiss.
Plate 23: Streaky grey gneiss sublithology of the Granitic gneiss map unit.
Plate 24: Photomicrograph of recrystallised plagioclase in weakly foliated amphibolite.
Plate 25: Photomicrograph of meta-peridotite.
Plate 26: Photomicrograph of Megacrystic gneiss quartz ribbon.
Plate 27: Photomicrograph of Megacrystic gneiss K-feldspar megacryst.
Plate 28: Photomicrograph of Megacrystic gneiss K-feldspar megacryst.
Plate 29: Photomicrograph of Megacrystic gneiss porphyroblast rimmed by subidioblastic epidote.
Plate 30: Photomicrograph of poikiloblastic garnet in biotite-garnet schist.
Plate 31: Photomicrograph of stained thin sections of felsic 'mylonitic' gneiss.
Plate 32: Thin section of spaced asymmetric crenulations.
Plate 33: Thin section of Megacyotic gneiss (XY section).
Plate 34: Photomicrograph of deformation banding in quartz ribbons.

Chapter 1
Introduction

1.1 Location of the study area

The study area is located within the eastern Harts Ranges, approximately 150km ENE of Alice Springs in the Arunta Inlier, central Australia. Detailed mapping was carried out over an area of 32km^2, immediately southeast of Spriggs Creek Bore, along the western margin of the Entia Dome. The semi-arid terrain is of moderate to low relief cut by intermittent, sandy creeks. The sparse vegetation is dominated by grasses and *Spinifex* with dense *Acacia, Eucalyptus* and *Melaleuca* near watercourses. Access to the area (located on the pastoral lease of Ambalindum), was via Claraville station to the southwest or from the Plenty Highway to the north.

1.2 Previous Investigations

The Harts Range, located within the eastern section of the Arunta Inlier, is considered to be a typical example of the intracratonic, polymetamorphic mobile belts characteristic of Proterozoic terrains (Plumb et al., 1981). The Inlier consists of mafic, felsic and bimodal meta-igneous rocks with abundant silicic, aluminous and calcareous metasediments. There has been systematic regional mapping of parts of the Arunta Inlier since the late 1960's and in order to synthesise the data, the Bureau of Mineral Resources, Geology and Geophysics (BMR), developed the Division-Province concept (Shaw & Stewart, 1975; Shaw et al., 1984; Stewart et al., 1984).

The rocks of the Harts Range area, defined as the Harts Range Group by Joklik (1955), have been assigned to Division 2/Central Tectonic Province by Shaw et al, (1982). The recent publication of the 1:250 000 Illogwa Creek Geological Sheet defines the Harts Range Group as comprising the quartzofeldspathic Entia and Bruna Gneisses and the concordantly overlying, pelitic Irindina and Brady Gneisses, (Shaw & Freeman, 1985). They propose that these Division 2 formations overlie the Division 1 Strangways Metamorphic Complex with a discordant boundary which is presumed to be a deformed unconformity, now represented by a 'tectonic slide'.

Detailed mapping by Buick (1983), Ding and James (1985), Foden (1985) and Lawrence et al (in press) in the Harts Range and Entia Dome has led to a reappraisal of the published classification scheme (figure 1.1). On the basis of igneous and metamorphic characteristics and structural style, they propose that the Entia Dome lithologies be designated 'basement' (i.e. a structural equivalent to the Division 1 Strangways Metamorphic Complex). The 'Entia gneiss

complex' is juxtaposed along large scale thrusts with a meta-pelitic 'cover' that includes the 'Harts Range meta-igneous complex' within the 'Irindina supracrustal assemblage', (Ding & James, 1985; Sivell & Foden, 1985). The Bruna gneiss occupies a restricted position between basement and cover and is described as being a later, thrust controlled intrusive that has been variably mylonitised, (Ding & James, 1985).

Study is continuing in this interesting region that includes both the 'basement' and 'cover' lithologies in order to understand their separate origins and development as well as the timing of their juxtaposition and subsequent deformation. These studies may, in turn, help unravel the complex tectonostratigraphic history of the Arunta Inlier, and provide an insight into the geological environments of the Early to Middle Proterozoic.

1.3 Aims of this project

1. To produce a geological map at the scale 1:12 500 of the area.
2. A detailed study of the regional, minor and microscopic structures and fabrics.
3. A qualitative and quantitative analysis of strain development in the study area.
4. To suggest a tectonic history of the area with special emphasis on the Bruna gneiss, and to comment on the significance of this to the region.

1.4 Methods

1. Four colour aerial photographs of 1:25 000 enlarged to approximately 1:12 500 black and white prints, were mapped on foot.
2. Approximately 40 thin sections were described with modal analyses carried out on most representative samples.

All thin sections and hand specimens are prefixed by 865- and are located in the Department of Geology and Geophysics, University of Adelaide.

Figure 1.1: Geological and tectonic map of the Harts Range area from James & Ding (in press). Study area is coloured, note extent of the Bruna gneiss.

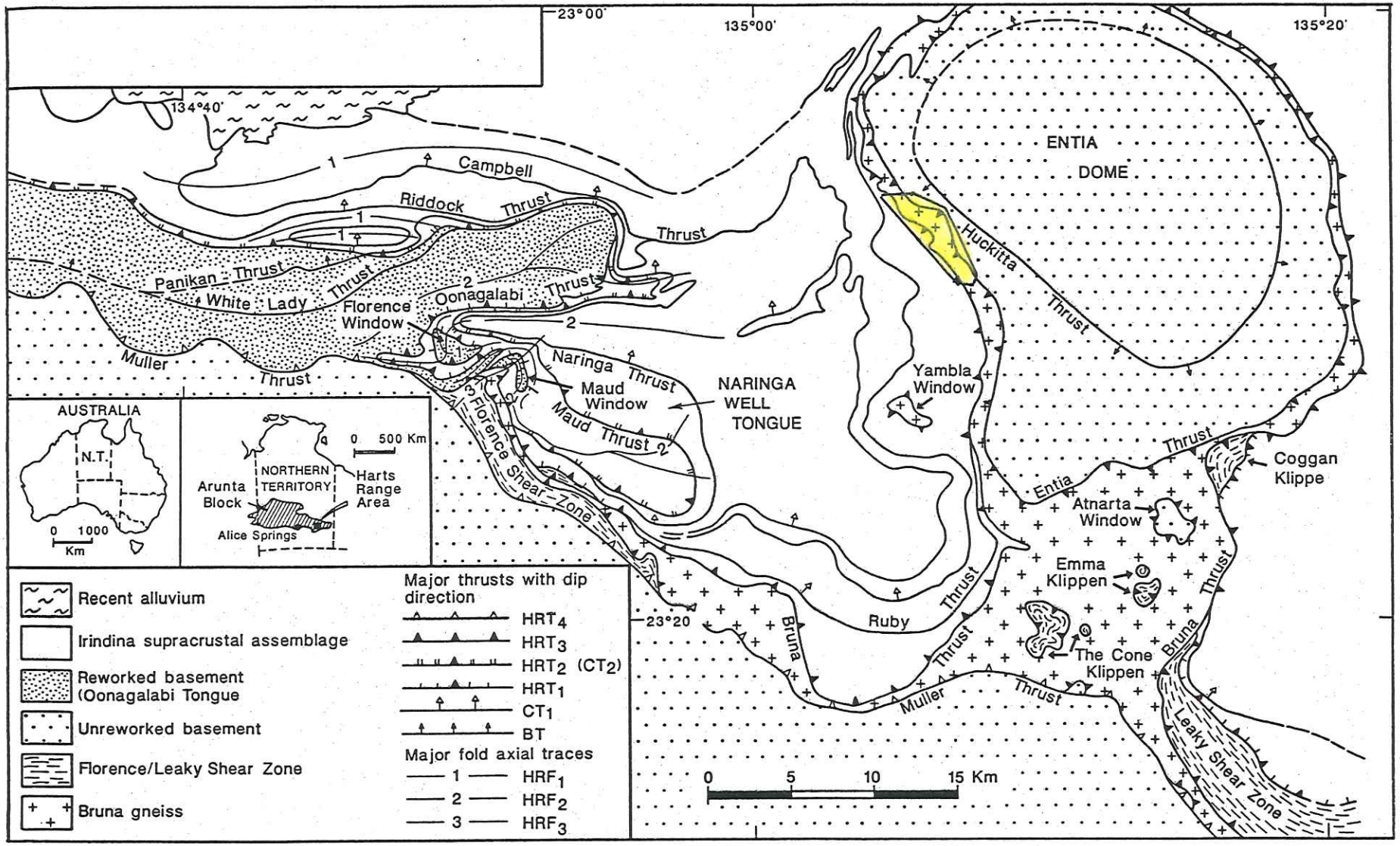
23°00'
135°00'
135°20'
134°40'
23°20'
ENTIA
DOME
Campbell
Riddock
Thrust
Panikan Thrust
White Lady Thrust
Florence Window
Oonagalabi Thrust
Muller Thrust
Naringa Thrust
Maud Window
Maud Thrust
NARINGA WELL TONGUE
Florence Shear Zone
Huckitta Thrust
Yambla Window
Entia Thrust
Coggan Klippe
Atnarta Window
Emma Klippen
The Cone Klippen
Ruby Thrust
Bruna Thrust
Muller Thrust
Leaky Shear Zone
0 5 10 15 Km
AUSTRALIA
N.T.
0 1000 Km
NORTHERN TERRITORY
Arunta Block
Harts Range Area
Alice Springs
0 500 Km
Recent alluvium
Irindina supracrustal assemblage
Reworked basement (Oonagalabi Tongue
Unreworked basement
Florence/Leaky Shear Zone
Bruna gneiss
Major thrusts with dip direction
HRT4
HRT3
HRT2 (CT2)
HRT1
CT1
BT
Major fold axial traces
1 HRF1
2 HRF2
3 HRF3

Chapter 2
Description of Lithologies

2.1 Introduction

The study area includes rocks of the Entia gneiss complex, the semi-pelitic lithologies of the Irindina supracrustal assemblage, and the Bruna gneiss (Ding & James, 1985) (figure 1.1). A geological map of the study area, at a scale of 1:12 500 is shown in figure 1. Lithological variation occurs from thin section to outcrop scale, therefore map units (described in figure 1) were defined using the following criteria:

- mineralogy of component lithologies
- relative abundance of each lithology
- textural characteristics, including small scale structures and fabric development

The field relationships and petrography of the major lithologies are described in sections 2.2, 3, 4 and a brief summary of metamorphic conditions in section 2.5. Representative thin sections are described in Appendix II.

2.2 Lithologies of the Entia gneiss complex

2.2.1 Quartzofeldspathic gneiss

This medium to coarse grained, granoblastic gneiss outcrops along the northern margin of the map area and occupies approximately 80% of the 'Grey gneiss' map unit. Weathering to orange and pale grey, low flaggy outcrops, this lithology has also been described by Sullivan, (1985) (plate 2). It is composed of granoblastic, inequigranular quartz (50-70%), K-feldspar and plagioclase (5-40%) pleochroic brown to green biotite (5-25%), with variable muscovite. A penetrative foliation is defined by evenly distributed fine to coarse mica and a fine (1-10cm) compositional banding of alternating biotite rich and poor layers. Irregular, (less than 5cm) concordant sills of coarsely crystalline quartz/feldspar aggregates and 0.5-5mm thick streaks of decussate biotite sheaths become more common as this lithology grades into the structurally overlying 'Migmatite' map unit (plate 3). The origin of this gneiss is uncertain, it may represent an original arkosic sediment within a supracrustal sequence, or it may have been emplaced into metasediments as a granitic intrusive.

2.2.2 Kyanite-biotite schist

A distinctive, 0.5-2m thick, crenulated kyanite-biotite(phlogopite?)-quartz schist is included within the Quartzofeldspathic gneiss. Grey/green to deep blue kyanite prisms (1-10cm long) and clear granular quartz are wrapped by coarse sheaths of faintly pleochroic biotite/phlogopite?. The kyanite appears irregularly oriented but is broadly parallel to the mica foliation. The gradation from aluminosilicate bearing schist to quartzofeldspathic gneiss is marked by a migmatitic zone (approximately 1m wide) of chaotically folded, streaked out segregations of very coarse quartz + feldspar + biotite clots and small (less than 10mm) kyanite blades. The kyanite schist is discontinuous, unlike its migmatitic envelope which can be traced northwards. This lithology may have developed from a pelitic metasediment subsequently affected by metamorphic differentiation.

2.2.3 Layered amphibolites

Layered amphibolites, characterised by alternating 1-40mm thick mafic/-leucocratic banding are intercalated with calc-silicates, felsic and granitic gneisses in all map units within the Entia gneiss complex (plate 1). The numerous, tabular outcrops, varying in thickness from 10cm to 15m are generally ellipsoidal and discontinuous but conformable (with sharp contacts) within their enclosing host lithologies. They form resistant black, to reddish brown bluffs and dip-controlled slopes that can be traced along strike for up to approximately 400m. The layered amphibolites occupy approximately 60% of the 'Layered amphibolite' map unit, and form a significant component (in terms of cumulative volume) of the Entia gneiss complex within the study area.

Their mineralogy and textures are highly variable and gradational, however the following sublithologies define their compositional banding:

1. Mafic layers with up to 90% elongate, pleochroic yellow-green to blue green hornblende of variable grainsize, (0.1-10mm) as aligned subhedral rhombs and/or recrystallised aggregates. A variably developed S to L-S fabric, parallel to the compositional layering is defined by the shape preferred orientation of the amphibole. Fine grained, granoblastic, equigranular to elongate plagioclase, sphene, diopside, K-feldspar and minor opaques (ilmenite?), zircon and apatite are scattered throughout.

2. Well defined, persistent felsic layers (0.1–10cm thick) with approximately 80% medium grained, granoblastic polygonal plagioclase (plate 2f). The grains are typically equant and untwinned, with gently curving grain boundaries and non-equiangled triple point junctions. The feldspar becomes finer grained and elongate with increasing hornblende and diopside content.

3. Lensing aggregates (less than 15mm wide) of medium to coarse grained pla-

gioclase and K-feldspar occur sporadically, parallel to the leucocratic banding. The coarse, irregular feldspars are strain shadowed with lobate to serrate grain boundaries. Very fine grained, elliptical grains of quartz or feldspar are scattered along grain boundaries.

The internal compositional layering is broadly concordant with the amphibolite margins and the foliation of adjacent gneisses; it occasionally cuts amphibolite-gneiss contacts at very low angles and is commonly tightly folded within thicker (greater than 40cm) layered amphibolite outcrops, (plate 9). The origin of the amphibolites is discussed in section 2.2.9.

2.2.4 Calc-silicates

Lithologies with calc-silicate mineralogy are commonly associated with the layered amphibolites, usually forming resistant, discontinuous slabby outcrops readily identified by their regular banding and pink/green colouration. The calc-silicates outcrop in all map units, although their relative abundance is difficult to estimate due to their discontinuous and gradational nature. Competence contrasts between component layers has resulted in spectacular boudinage and folding of the layering during deformation.

Like the amphibolites, the calc-silicates have a highly variable mineralogy and field appearance, and several lithological types have been recognised:

1. Mafic calc-silicates occur concordantly within or adjacent to layered amphibolites. They consist of alternating, essentially monomineralic laminae, (0.1-2mm) of ribbon quartz, epidote, clinozoisite, hornblende and granular scapolite, (plate 34). Sphene, diopside and skeletal clinopyroxene, (augite?) are commonly present.

2. Calc-silicate gneisses consisting of regular layers (2–30mm) of medium grained granoblastic quartz, pink K-feldspar and muscovite wrapping spindle shaped boudins (10–30cm) of phaneritic hornblende and/or epidote, and quartz.

3. Spotted calc-silicates consisting of knobbly, quartzofeldspathic segregations up to 50cm wide that include large, scattered crystals of hornblende.

4. Brecciated calc-silicates consisting of intensely fractured, massive epidote + hornblende permeated by anastomising veins of prismatic quartz + calcite. These occur as isolated outcrops up to 5m in diameter in the southern region of the study area.

The calc-silicates may have been derived from calcareous marls, and/or metasomatic alteration of mafic igneous protoliths or volcanoclastic sediments (Stewart, 1985).

2.2.5 Massive amphibolite

Massive amphibolites form distinctive black lenses and irregular pods several metres in diameter. These lack any compositional banding although they commonly have a variably developed lineation and foliation defined by nematoblastic amphibole and flattened, elongate aggregates of plagioclase. Massive amphibolites outcrop in all the major map units (notably common in the Lineated leucocratic gneiss map unit) and may be gradational into layered amphibolites or isolated as boudins within host gneisses.

The dominant mineral phase is pleochroic pale to deep green, sub- anhedral, simple twinned hornblende. Secondary hornblende and epidote commonly form fine grained aggregates and trails along primary hornblende cleavages and grain boundaries. Large skeletal remnants of augitic clinopyroxene, altered to finely striated, brownish patches occur throughout. Some hand specimens are a pudding-like mass of hornblende clots (approximately 2cm in diameter) that may have replaced coarse pyroxene crystals. Plagioclase frequently occurs as small aggregates of complexly twinned, sericitised, highly strained grains. Recrystallised, polygonal, strain-free grains also occur, especially between clinopyroxene and secondary hornblende.

Massive amphibolites containing remnant clinopyroxene may have initially been emplaced as clinopyroxenite sills into the supracrustal sequence (Stewart, 1985). Their association with the felsic gneisses of the Lineated leucocratic gneiss map unit is uncertain, although they may be genetically related to igneous protoliths (?) of the gneisses.

2.2.6 Felsic gneiss

This finely layered (0.5–5cm) felsic lithology is a cream to orange, medium grained, microcline rich granoblastic gneiss (plate 4), and is the major component of the Lineated leucocratic gneiss map unit. Elongate augen (up to 4cm in diameter), of pink microcline and rod-like quartz aggregates and ribbons produce a pervasive lineation. The felsic gneiss contains medium to fine grained, polygonal to irregular, crosshatched microcline (25–50%), mildly sericitised plagioclase (10–40%), and inequigranular lobate quartz (5–25%). Ragged pale yellow to dark brown lepidoblastic biotite (0–10%) and coarse, skeletal grains of muscovite are unevenly scattered throughout the gneisses.

2.2.7 Minor quartzites, schists and augen gneisses

Throughout all the map units are thin (10cm-3m) lenses and layers of various quartzose and schistose lithologies. Some of these minor rock types may represent meta-pelite/psammite sequences.

The quartzites are typically thin (5-30cm) cream to pale grey layers of coarsely crystalline quartz with minor microcline, muscovite and biotite as inclusions within the strain shadowed, serrate grains. These resemble the quartzose, component layers of the calc-silicates, however these minor quartzites are not associated with calcareous lithologies.

The schists are extremely variable in thickness and mineralogy. Distinctive dark brown and green schists occur as 1-3m layers within the Migmatite map unit. The chlorite schist contains rounded (2cm) plagioclase augen in a medium grained matrix of decussate chlorite sheaths wrapping lozenge shaped aggregates of strongly sericitised plagioclase and quartz. Small, subhedral to ragged, twinned epidote grains are uncommon. The dark brown schists vary from pure coarse biotite to crenulated, quartz-biotite schists crowded with coarse quartzofeldspathic augen.

Augen gneisses occur sporadically throughout the area. These outcrop as prominent discontinuous bands 20cm–1m wide, with some appearing to be sheared, layer-parallel pegmatites (due to their mineralogy and grainsize). The mineralogy is variable but usually includes very coarse, pink and grey perthitic K-feldspar augen wrapped by quartz ribbons and finely recrystallised granoblastic feldspar. An anastomising, spaced fracture cleavage has typically developed within thick (>1m), homogeneous, medium to coarse grained quartzofeldspathic layers.

2.2.8 Meta-ultramafic rocks

In the centre of the map area, close to the contact between the 'Lineated leucocratic gneiss' and Granitic gneiss map units, is a low elliptical hill approximately 400m in diameter composed of meta-ultramafic and mafic lithologies. The dark outcrop is massive in parts, particularly near its southeastern margin, but elsewhere has a weak schistose fabric. The massive section is composed of meta-peridotite with large (2–6mm) irregular oikocrysts of pale green clinopyroxene containing numerous, ragged to subrounded, strongly fractured olivine grains. Occasional highly altered plagioclase remnants are bordered by radiating aggregates of finely recrystallised augite(?) and plagioclase(?). The fine, pale green matrix has pseudomorphed all the major mineral phases (plate 25). Other lithologies within this outcrop include deformed metahornblendite with coarse grained lithologies that have been kinked and recrystallised; and altered sericitic and chloritic amphibolite.

The subcircular shape of this outcrop and clear igneous textures indicate this intrusive has not experienced a similar intensity of deformation of the surrounding units. However it does not appear to crosscut lithologies; the gneisses and amphibolites wrap around the outcrop. Prominent, vertical pegmatites cut the intrusive and abruptly terminate at the contact with the Bruna gneiss.

2.2.9 Origin of the Entia gneiss complex lithologies

The Entia gneiss complex (part of the Strangways Orogenic Belt (James & Ding, in press)) has been informally grouped into two series: a supracrustal component consisting of para- and orthoamphibolites, calcareous and quartzose pelite/psammite sequences; and an intrusive component of granitic to tonalitic orthogneisses (Foden & Buick, 1986). Within the study area, the apparent association and conformity of layered amphibolites with calc-silicates suggest their development was closely associated with sedimentary accumulation, and at least some of the mafic lithologies may be para-amphibolites (Sills & Tarney, 1984) Although original intrusive and sedimentary relationships have not been recognised in this field study, the predominance of the amphibolites, particularly in the Layered amphibolite map unit, suggest an igneous origin for most of the amphibole bearing lithologies. These orthoamphibolites probably originated as basaltic flows and pyroxenite - amphibolite sills (Goscombe, 1984; Stewart, 1985) emplaced into the calcareous and semi-pelitic metasediments. The fine leucocratic banding within the layered amphibolites may have been produced by subsequent metasomatic differentiation mimetic after a primary igneous/sedimentary layering. Similar textures produced by tectonic thinning of basalt pillow structures have been described by Myers (1984).

The origin of the quartzofeldspathic and felsic gneisses of the study area is unclear. They may also have been part of the supracrustal sequence as arkosic metasediments, although occasional, low angle discordances between the internal amphibolite banding and the gneiss/amphibolite contacts suggest the gneiss protoliths intruded into metasediments, subparallel to the layering. However, such discordances may also have developed due to competence-contrast induced deformation (such as boudinage).

The Migmatite map unit (consisting of chaotically folded and lensing migmatitc banding of all lithologies) is interpreted as having formed by migmatitic differentiation of both the Grey gneiss and Layered amphibolite map units. The kyanite-biotite schist and its migmatite envelope are believed to have formed during this peak metamorphism with partial melting of the quartzofeldspathic gneiss, producing an aluminosilicate-bearing restite (Sullivan, 1985; Oliver & Foden, 1986).

2.3 Bruna gneiss

The Bruna gneiss, as mapped by the BMR and others, outcrops as a continuous layer that can be traced between the 'cover' and 'basement' lithologies for a considerable distance (figure 1.1). Significant mineralogical and textural variation occurs within the Bruna gneiss, (Joklik, 1955; Martin, 1983; Rankin, 1983), and this study subdivides the gneiss into two units; the Granitic gneiss and Megacrystic gneiss (figure 1).

The Granitic and Megacrystic gneisses within the study area are broadly concordant with the structurally underlying Entia gneiss complex and overlying Irindina supracrustal assemblage lithologies. However, elsewhere the Granitic gneiss has been observed to cross cut major 'basement' boundaries and structures, (Parker, in prep; Ding & James, 1985). The lateral persistence of the gneiss led early workers to interpret its origin as feldspathic sediment (Joklik, 1955). The extensive, discordant nature of this lithology, its texture, composition and the inclusion of xenoliths has led to the recent interpretation of the Bruna gneiss as a thrust controlled, porphyritic intrusive, (Ding & James, 1985).

2.3.1 Granitic gneiss

The Granitic gneiss is the major lithology within the Bruna gneiss, corresponding to the 'even grained acid gneiss' of Joklik (1955), and 'lower unit' of Martin, (1983). It weathers to resistant, orange-brown, boulder-strewn hills and pavements, and hosts prolific *Spinifex* growth! The unit is very heterogeneous due to compositional and grainsize variation, predominantly with alternating layers (3cm-2m wide) of even grained and augen bearing quartzofeldspathic gneiss, (plate 20). The coarser grained and augen bearing layers display an intense lineation, defined by elongate, flattened feldspar megacrysts, biotite and attenuated garnet and hornblende aggregates, (plate 8). Other lithologies occurring within this unit include:

- Fine grained, grey amphibole-rich streaky gneiss close to the upper boundary. It contains small (1-10cm), streaked out mafic schlieren which most likely represent deformed xenoliths (plate 23).
- An uncommon medium grained, orange-pink, relatively undeformed (*ie* only weakly lineated) granitoid, occurring as discontinuous 1m wide lenses.
- Thin (less than 20cm) lenses of muscovite rich quartzite and very coarse grained augen gneiss. These small schistose outcrops are commonly cut by numerous, finely striated, curved epidote-rich surfaces that resemble slickensides.
- An irregular, 50 metre wide mass of contorted calc-silicate, believed to be a large deformed xenolith from the 'basement' gneisses.
- Rare discontinuous mafic lenses up to 1m long, conformable with the gneissic layering, also interpreted as amphibolite xenoliths from the 'basement'.

The Granitic gneiss is interpreted as a porphyritic, granitic intrusive emplaced into an active shear zone, (Ding & James, 1985; James & Ding, in press) It is probable that a primary foliation developed whilst it was still partially molten ((Gapais & Barbarin, 1986) and (P. Ding, pers comm)) due to intense shear stress. An initial compositional layering may also have developed during cooling and partial assimilation of xenoliths.

2.3.2 Megacrystic gneiss

The Megacrystic gneiss is a relatively thin unit (approximately 130m thick) structurally overlying the Granitic gneiss. It is distinctive in the field, weathering to chocolate brown, schistose, rubbly outcrops. It was first described by Joklik as a Bruna gneiss variant containing microcline and blue-grey andesine augen. This unit has also been described as the 'upper unit' of the Bruna gneiss by Martin (1983), and has recently been interpreted as a mylonitised zone derived from the underlying granitic lithologies (Lawrence, in prep).

Compared with the Granitic gneiss, the Megacrystic gneiss is relatively homogeneous, with larger K-feldspar and plagioclase augen up to 5cm in diameter. It consists of K-feldspar (20-30%), plagioclase (20-35%), brown to green biotite (10-30%) and less common hornblende, garnet, sphene, allanite and opaques. The megacrysts are predominantly single, subrounded, polysynthetically twinned or microperthitic grains and elongate polycrystalline aggregates. Minor augen are comprised of quartz, poikiloblastic garnet and green amphibole. The feldspar and quartz megacrysts display internal plastic deformation, with undulose extinction, twinning and advanced subgrain formation. Mortar texture is well developed, along with myrmekitic patches and recrystallised new grains surrounding the augen (plate 27).

The Megacrystic gneiss has a strongly developed L-S tectonite fabric (Turner & Weiss, 1963), with the foliation formed by flattened megacrysts, lepidoblastic biotite and quartz sheets. The lineation is defined by elongate aggregates and aligned hornblende prisms, as well as by the intersection of the foliation and biotite deflected around augen (plate 22).

2.4 Irindina supracrustal assemblage

The Irindina supracrustal assemblage within the study area is composed mainly of garnet bearing, interlayered biotite schists and amphibolites, with minor impure marbles, calc-silicates and felsic gneisses. This extensive assemblage (figure 1) has been interpreted as a mixed volcano-sedimentary cover sequence, its dominant layering and foliation having developed during an upper amphibolite facies, tectonothermal event (Sivell & Foden, 1985).

2.4.1 Amphibolite

The lower boundary of the Irindina assemblage (in contact with the Megacrystic gneiss), is abruptly marked by mafic amphibolite of variable mineralogy and structure. This lithology may be up to 10m thick, although it usually outcrops as a 1-3m wide contorted lens of finely layered amphibolite (plate 7). The mineralogy is essentially that of layered amphibolites described previously but also includes a

significant amount of porphyroblastic garnet. Pure calcite and calc-silicate layers (2-20cm wide) are also present. At one locality, thin (15cm) black mafic 'sills', concordant (and interleaving) with the Megacrystic gneiss, mark the contact. These appear to be sheared amphibolite, with strongly aligned, marginally recrystallised hornblende rhombs, polygonal plagioclase and abundant equant opaques. The green hornblende has been partially recrystallised to fine, pale green (slightly less Fe rich?) new grains and associated magnetite(?).

2.4.2 Biotite-garnet schists

The pale grey to black biotite schists are irregularly layered, well foliated with pleochroic green to dark brown biotite (20–40%), very pale pink garnet (5–40%), plagioclase (20–50%), quartz (5–15%) and minor green hornblende, opaques and sphene. These commonly contain rotated boudins of finely laminated amphibolite, (figure 3.3d), as well as coarse seggregations of quartz and large (up to 10cm in diameter) poikiloblastic, fractured garnet. Patchy sillimanite was observed in several outcrops.

2.4.3 Impure marble

A 3m thick, impure marble with numerous, contorted boudins of various calc-silicate lithologies outcrops at the western margin of the map area, (plate 6). The pale green, coarsely crystalline marble consists of distinctively twinned calcite (50–70%), quartz (10%), epidote/clinozoisite (15–25%), K-feldspar, muscovite and sphene.

2.4.4 Felsic megacrystic and mylonitic gneisses

Thin (15cm) bands of pinkish grey mylonites occur near the base of the Irindina sequence. These are very fine grained (less than 0.5mm), with a granoblastic elongate matrix of quartz (30-40%), K-feldspar (20-25%) and plagioclase (20-40%). Small (0.5mm) plagioclase augen (with ragged, K-feldspar tails) and extremely attenuated garnets are wrapped by reddish brown biotite and quartz ribbons (plates 31 & 32).

A spectacular, lensing (0.3-2m thick) megacrystic gneiss is associated with the basal amphibolite. It consists of pebble-like to tabular, blue grey K-feldspar augen up to 10 cm in diameter, with paler, finely recrystallised margins and asymmetric tails. The augen are crowded within a quartzofeldspathic matrix that includes fine grained bioitite and mafic stringers.

2.5 Metamorphic Conditions

Previous investigations have suggested regional metamorphism of the Entia gneiss complex lithologies peaked at upper amphibolite- (Sullivan, 1985; Oliver & Foden, 1986) to transitional granulite facies (Shaw & Freeman, 1985; Ding & James, 1985). Evidence of local partial melting (plus granitic intrusions) associated with this thermal peak is observed throughout the Entia Dome (Buick, 1983; Foden & Buick, 1986). The presence of chlorite schist and minor subidioblastic epidote may indicate a patchy occurrence of retrograde metamorphism.

The rocks of the Irindina supracrustal assemblage have also been assigned to upper amphibolite facies (Sivell & Foden, 1985), although the presence of sillimanite (*cf* kyanite), the relative weak migmatisation and scarcity of granitic intrusives suggests the peak metamorphic event involved slightly lower pressures/temperatures in relation to the Entia Dome (Ding & James, 1985).

Plate 1: Typical brownish-orange outcrop of the Layered amphibolite map unit. The amphibolite is intimately interlayered with lensing quartzofeldspathic gneisses. (Scale bar is $1m$).

Plate 2: Flaggy outcrop of quartzofeldspathic gneiss within the Grey gneiss map unit. The coarsley crystalline quartzofeldspathic segregations become more common as this lithology grades upwards into the migatite gneisses of the Migmatitic map unit. (Scale is $30cm$.)

Plate 3: Irregular migmatite banding within the Migmatitic map unit. Strings and clots of biotite alternate with coarsely crystalline quartzose and feldspathic segregations. (Scale is $10cm$.)

Plate 4: Felsic gneiss of the Lineated leucocratic gneiss map unit. The ubiquitous lineation is defined by rod-like quartz aggregates and elongate microcline augen. (Scale is $10cm$.)

Plate 5: Isoclinal, class 2, recumbent EF_3 folds within the Layered amphibolite map unit. Note axial planar spaced fracture cleavage within leucocratic hinges. (Scale is $10cm$.)

Plate 6: Diffuse, rotated boudins of calc-silicate (honblende and epidote rich boudins are dark, spotted quartzofeldspathic blebs are white) within the impure marble of the Irindina supracrustal assemblage lithologies. (Scale is $30cm$.)

Plate 7: typical lensing, discontinuous layered amphibolite that outcrops along the upper (structural) boundary of the Megacrystic gneiss. (Scale is $30cm$.)

Plate 8: Feldspathic augen bearing layer of the granitic gneiss. XY section illustrating the steep, westward plunge of the lineation due to BF_3 folding. (Scale is $30cm$.)


1


2


3


4

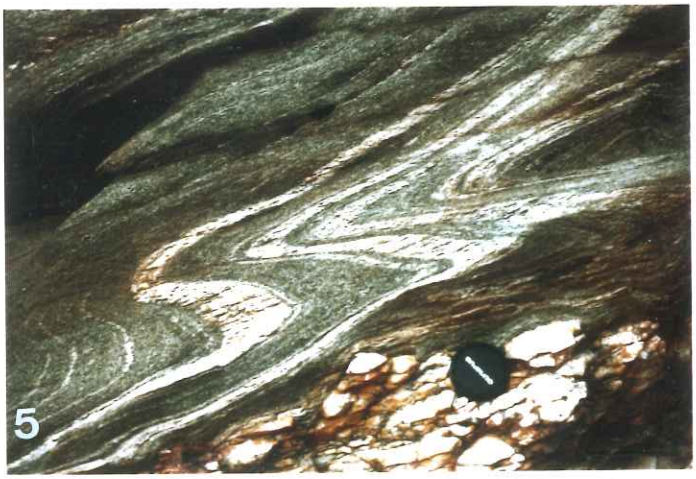
5


6


7


8

Chapter 3
Structural Relationships

3.1 Introduction

Previous investigations have recognised a complex interaction of intrusive igneous, metamorphic and ductile deformation events that have separately affected the 'basement' and 'supracrustal' sequences (Ding & James, 1985; Foden, 1985; James & Ding, in press). The extent to which the two terrains are genetically related, the timing and nature of their juxtaposition, and the somewhat enigmatic origin of the Bruna Gneiss are problems currently under investigation. This study groups the map lithologies into three, distinct sequences on the basis of structural and lithological characteristics (and follows previous classification) - namely the Entia (E), Bruna (B), and Irindina (I) lithologies, see figure 1. The aim of this structural analysis is to summarise the deformation events within the three groups, and to determine to what extent their structural development is related.

3.2 Methods and Terminology

Structural nomenclature and classification as outlined by Hobbs et al (1976) and Ramsay (1967) are used throughout this thesis (see AppendixIII). The prefixes I, B, and E are used to differentiate the deformational histories of the three major groups; for example EF_2 refers to the second fold generation observed in the Entia gneiss complex. Three subareas (I, II, III) have been identified on the basis of lineation and foliation trends (figure 3.1). Intense, repeated ductile deformation and the moderate to high metamorphic grade (including migmatisation) has resulted in layer parallel fabrics with a paucity of overprinting criteria. Detailed form mapping of key localities and stereographic projection of data have been necessary to determine some structural relationships.

3.3 Structures of the Entia gneiss complex

3.3.1 First Deformation ED_1

The earliest observable fold generation (EF_1) within the Entia gneiss complex is represented by low amplitude (less than 15cm) recumbent isoclinal folds that fold the compositional banding of the layered amphibolites, (plate 9) The angular, chevron or rounded, hinge thickened class 3 folds are often intrafolial and transposed, occurring only within the thicker (greater than 30cm) amphibolite layers. A layer-parallel, planar fabric defined by nematoblastic hornblende is weakly folded and disrupted within the EF_1 fold hinges indicating its pre ED_1 origin. Scattered

elongate hornblende grains within the leucocratic layers, and discontinuous quartz veins are oriented axial planar (figure 3.3a) to EF_1, thereby defining a nonpenetrative ES_1 fabric.

3.3.2 Second Deformation ED_2

The peak metamorphic event that migmatised and differentiated these lithologies to produce the regional gneissic banding ES_2, is interpreted as the second deformation phase ED_2. Numerous small (amplitudes less than 30cm), recumbent intrafolial folds exhibit gross hinge thickening and disruption where quartzose and feldspathic segregations have been emplaced. Flame-like structures, crosscutting veins, disharmonic folds and elongate mafic boudins are common within the irregular compositional layering, (plates 3 & 11). A pervasive fabric defined by lepidoblastic micas also developed in the quartzofeldspathic and felsic gneisses, which suggests their protoliths were present (emplaced?) within the supracrustal pile pre-syn ED_2.

3.3.3 Third Deformation ED_3

The third deformation (ED_3) involved close to isoclinal folding of the pervasive ES_2 gneissosity. Layers of varying competence were deformed differently, with the amphibolites often boudinaged and disrupted within the EF_3 hinges, and the thinner leucocratic and calc-silicate layers buckling into numerous ptygmatic folds. Macroscopic closures were only observed in two localities, buckling the relatively thick (greater than 40cm) lenses of amphibolite into inclined or recumbent tight folds, the hinges plunging gently toward $150° - 176°$ (magnetic north: MN) (plate 15).

The more finely layered lithologies display tight to isoclinal, class 2, recumbent EF_3 folds generally plunging $1° - 20°$ toward $150° - 260°$ (MN) (figure 3.2a). Strain analysis of flattened, parallel EF_3 folds within the Lineated leucocratic gneiss unit (see Appendix III)indicate total flattening strains of 59% to 77%. It is not possible to determine if flattening of these folds occurred during ED_3 or later deformations.

Axial planar ES_3 fabric development appears restricted to fold hinges within coarse grained leucocratic folds, with uncommon development of a spaced fracture cleavage (plate 5). Re-orientation of mica flakes into parallelism with EF_3 fold axial planes occurs in the quartzofeldspathic and felsic gneisses. However this fabric is only clearly observed at the thin section scale, and within fold limbs ES_3 foliations parallel the ES_3 gneissic layering. This combined ES_2/S_3 layering dips moderately southward (figure 3.1) and at the outcrop scale is warped by subsequent fold generations.

3.3.4 Fourth Deformation ED_4

Mesoscopic, s-vergence folds (EF_4), observed only in suitably oriented exposures along the eastern margin of subarea II, developed during the fourth recognizable deformation phase of these Entia lithologies. The hinges of these folds outcrop over several metres (plate 16) and can be just distinguished on the 1:25 000 colour aerial photographs. Closing to the south the ES_2/S_3 layering is tilted to vertical or slightly overturned by the EF_4 folds, trending 060° – 080°. Isoclinal EF_3 folds are refolded by EF_4 folds (plate 13). Lenticular and boundinaged layering where traceable around the EF_4 structures are strongly rotated (plate 14) or buckled (plate 12) indicating compressive stress has acted perpendicular to the fold axial plane. The limbs of the EF_4 folds also display limited evidence of extension parallel to the layering. One locality displays a 1.5m thick quartzose unit, bounded by layered amphibolite, cut by several steeply inclined dextral faults (figure 3.3b). The unit appears brecciated, with fine reticulate partings of weathered mica pervading the layer. The amphibolites are sheared parallel with and adjacent to the upper and lower contacts, and gently fold into the 'quartzite' where it thins due to the faults. This structure appears to have developed as the result of the two lithologies responding differently to imposed stress. The quartzite is behaving more competently, with extension being permitted by faulting and shearing (within the unit and along its margins). The EF_4 asymmetric folds are considered 'parasitic' on the limb of a much larger recumbent structure closing to the south.

3.3.5 Fifth and Subsequent Deformations

At least one, and possibly more periods of relatively low intensity deformation produced open, upright folds that trend east-west and north-south. The interference fold pattern produced is one of broad gentle domes and troughs throughout the area (plate 17). Late stage, disruptive pegmatitic intrusions are particularly common in the southern section of the study area.

3.4 Structures of the Bruna gneiss

3.4.1 First Deformation BD_1

The earliest folds (BF_1) observed within the Bruna gneiss only occur within the Granitic gneiss. A streaky, gneissic foliation is folded into faint small amplitude (less than 5cm) tight to isoclinal, recumbent intrafolial (BF_1) folds (plate 18). The fold hinges (of variable orientation) are angular and thickened, and megacrysts within them are extremely elongate parallel to the BF_1 axial planes. The foliation being folded by BF_1 is considered to be a pre-BD_1 fabric, with the more pervasive foliation intrafolialy enclosing defined BS_1 (as it is axial planar to BF_1). These folds are considered to resemble the B^m_m folds of Bell (1978).

3.4.2 Second Deformation BD_2

The second deformation identified within the Bruna gneiss is also only observed within the Granitic gneiss. Limited exposures of small (amplitudes up to 1m) recumbent, class 1c to class 2 folds are observed predominantly in subarea II, (plate 10). Thin pegmatitic layers within the gneiss have been folded by these BF_2 structures into numerous rounded closures (plate 19). The folded veins (or seggregations?) are commonly hinge thickened, disrupting and deflecting the pervasive fabric around them.

The ubiquitous lineation occurring throughout the the Granitic gneiss is not observed in the hinges of these BF_2 folds. Where it occurs away from the fold hinges, it is parallel on both the upper and lower limbs, trending at a high angle to the horizontal BF_2 hinge orientations, (figure 3.2b) unlike the orientation of lineation around later folds. It appears that these BF_2 structures formed during the formation of the L-S fabric, however their hinges have not been rotated into parallelism with the lineation and direction of shearing (Evans & White, 1984)

Within the hinges of some BF_2 folds, the foliation is tightly crenulated. The hinges of these small (less than 1cm) asymmetric and 'M' shaped structures produce a faint intersection lineation parallel with (and confined to) the fold hinge.

3.4.3 Third Deformation BD_3

The L-S fabrics of the Megacrystic and Granitic gneisses are folded by mesoscopic, upright to inclined BF_3 folds, producing localised linear regions within the hinge zones of steeply dipping foliation. These discontinuous regions are referred to as 'steep zones', and they can be traced along strike for up to 200m. The lineation is folded around BF_3 closures and plunges steeply to the west in the hinge zones (figure 3.1). These steep zones are essentially confined to subarea II where they dominate the outcrop structure, trending 070°-090° (MN) although the occasional BF_3 folds are observed in subarea III. A detailed analysis of the 'anatomy' of the BF_3 folds is given in figure 3.4.

3.4.4 Fourth Deformation BD_4

Evidence for the subsequent deformation of the BF_3 folds is observed in few localities. The BF_3 fold hinges (steep zones) are discontinuous, however in suitable exposures their hinges are observed to curve into open flexures with amplitudes of 3-10 metres. The axial planes of these rare BF_4 structures are slightly inclined towards the west and strike approximately 165° (MN) (figure 3.4).

3.4.5 Fifth Deformation BD_5

The fifth identifiable phase BD_5 produced folds that affect the upper boundary of the Megacrystic and the overlying 'cover' sequences. This contact is consistently folded into open, upright antiformal 'noses' plunging 0° — −20° towards 250° — −270° MN. These structures are observed only along the contact and appear to be masked by complex fold interference patterns away from it. They do not occur in the Granitic gneiss.

3.5 Structures of the Irindina supracrustal assemblage

3.5.1 First Deformation ID_1

The well foliated meta-pelites and amphibolites of this assemblage are almost flat lying within the study area, and it has not been possible to observe some of the complex structural features described elsewhere (Lawrence, in prep; Ding & James, 1985). The earliest fold generation recognised is represented by faint, disrupted isoclinal recumbent class 2 folds with amplitudes of 10cm to 30cm. These IF_1 structures, folding a barely distinguishable IS_1 (?) foliation, are disrupted by the pervasive schistosity that has developed actually planar to them (IS_2). The IS_2 foliation also contains elongate amphibolite boudins that have been rotated, their internal fine leucocratic laminations at a high angle to the surrounding IS_2 foliation (figure 3.3c).

3.5.2 Second Deformation ID_2

Structures formed by ID_2 appear to be related to relative movements of the 'cover' and the structurally underlying Megacrystic gneiss. Small (less than 50cm amplitude), asymmetric closures in the schists occur immediately adjacent to the contact. These uncommon IF_2 folds are of variable orientation and shape, and appear to be abruptly dragged into parallelism with the boundary. These folds are not observed away from this movement zone. Where layered amphibolite outcrops along the contact its layering appears contorted and rotated, giving a characteristic 'onion weathering' appearance (plate 7).

3.5.3 Third Deformation ID_3

The open upright BF_5 folds of the Megacrystic gneiss correspond to the third fold generation recognised in the Irindina lithologies (IF_3) (figure 3.1). Away from the basal contact with the Bruna gneiss the IS_2 foliation is flat lying, warped into low domes and basins as a result of fold interference patterns and subsequent low

intensity deformation. Large pegmatites, some more than 500m long, trending approximately E/W are common throughout this sequence.

3.6 Structural Summary

The relationships between deformational histories of the three sequences is summarised in table I, and a sketch of the major structural elements of the map area is given in figure 3.1. A change in orientation of the regional foliation from predominantly NW/SE to E/W defines a macroscopic 'kink band' of subarea II in which the steep zones are distinctive. Figure 3.6 illustrates the trend of lineations throughout the study area and the contoured dip of foliations (IS_2, BS_2, ES_2). These figures highlight the association of 'steep zones' with the abrupt change in lineation trend from south to west.

Many of the distinctive lineaments visible on aerial photographs and Landsat imagery do not appear to correspond to geological features. These major features with variable trend but predominantly NNW generally correspond to linear watercourses and gullies, and less commonly to pegmatites; however no faulting, fault breccia or linear intrusions have been correlated with them in this study area.

Table I

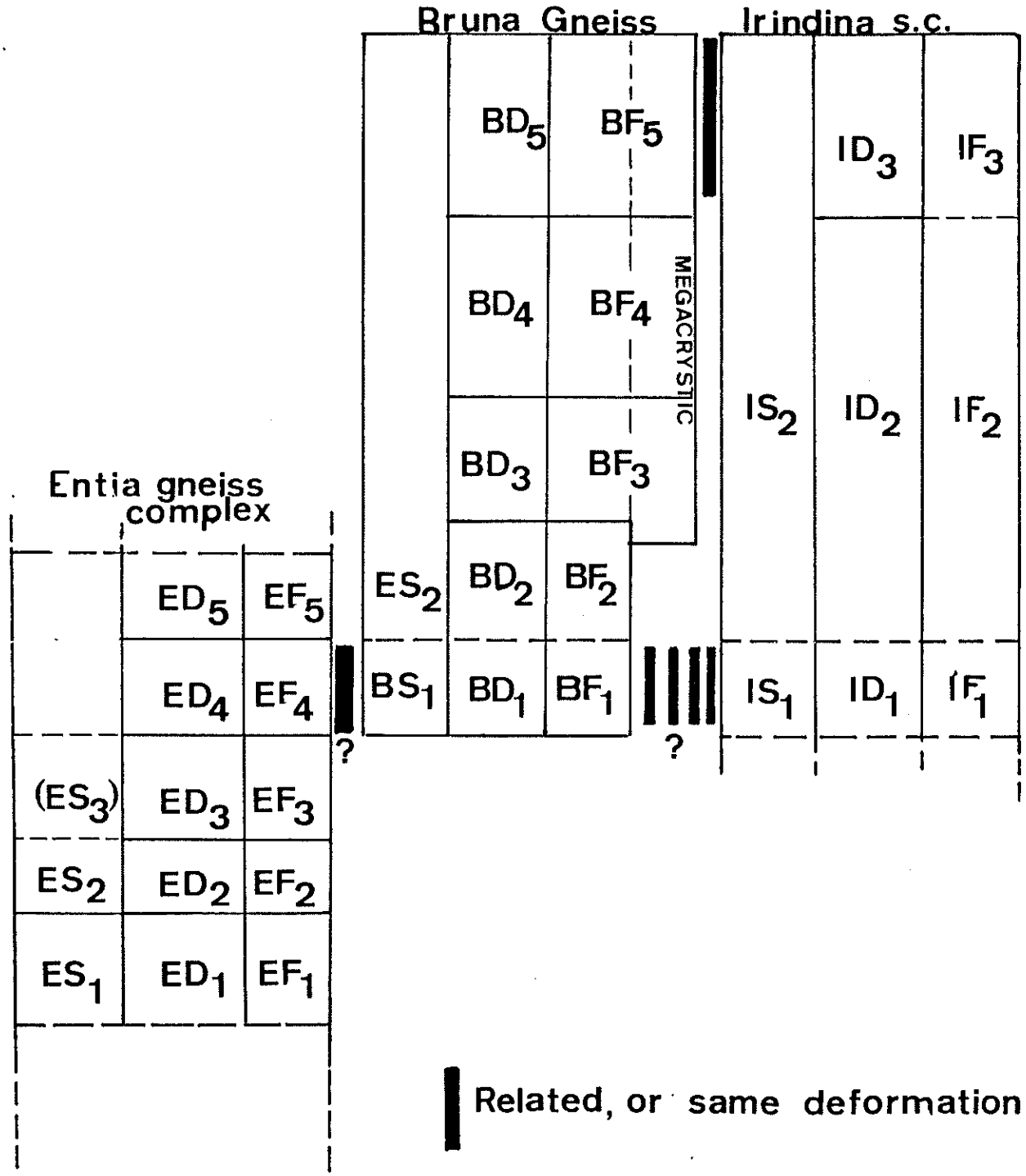
Bruna Gneiss
Irindina s.c.
Entia gneiss complex
BD5
BF5
ID3
IF3
BD4
BF4
MEGACRYSTIC
IS2
ID2
IF2
BD3
BF3
ED5
EF5
ES2
BD2
BF2
ED4
EF4
BS1
BD1
BF1
IS1
ID1
IF1
?
?
(ES3)
ED3
EF3
ES2
ED2
EF2
ES1
ED1
EF1
Related, or same deformation

Figure 3.1: Summary of the major structural elements of the map area. Note subareas I, II and III that correspond to a macroscopic 'kink' band in the regional foliation.

(a) Bruna gneiss, subarea II poles to the BS_2 foliation. Contoured density of 194 points, contours of 2.0, 5.1, 11.8, and 14.0% per 1% area.
(b) Bruna gneiss, subarea II lineations. Contoured density of 144 points, contours of 1.4, 2.8, 4.8, 5.5, and 11.1% per 1% area.
(c) Bruna gneiss, subarea III poles to the BS_2 foliation. Contoured density of 56 points at 1.8, 5.4, 12.5, and 17.9% per 1% area. Maximum 19.6%.
(d) Bruna gneiss, subarea III lineations.
(e) Entia gneiss complex, poles to the ES_2. Contoured density of 231 points at 0.65, 2.16, 4.7, 8.6, 12.9, 17.32, and 25.3% per 1% area.
(f) Entia gneiss complex lineations.

Arrows define the BF_5 fold hinges.

Figure 3.1

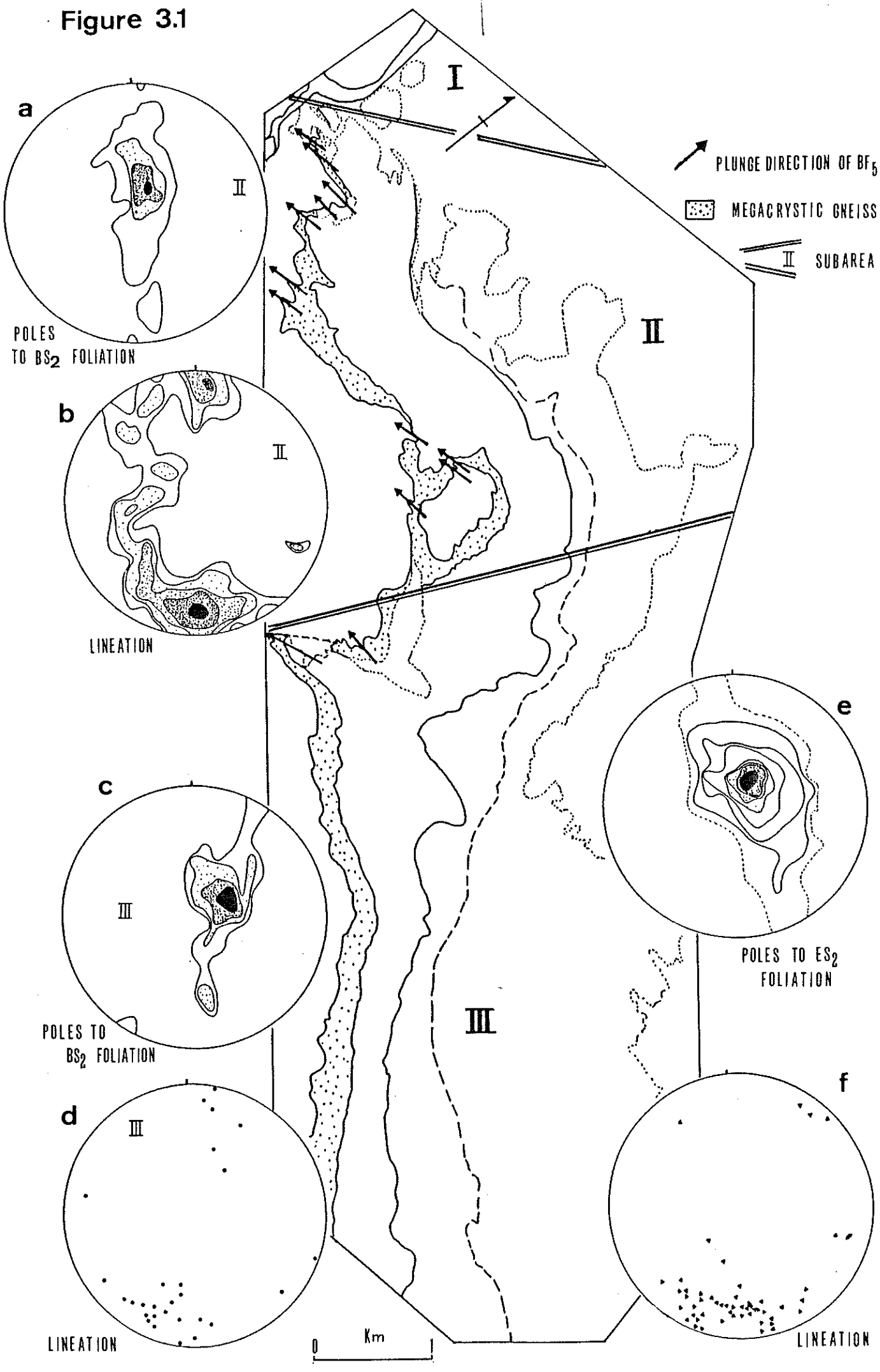
a
II
POLES
TO BS_2 FOLIATION
b
II
LINEATION
I
II
III
PLUNGE DIRECTION OF BF_5
MEGACRYSTIC GNEISS
II SUBAREA
c
III
POLES TO
BS_2 FOLIATION
d
III
LINEATION
e
POLES TO ES_2
FOLIATION
f
LINEATION
0 Km

Figure 3.2a: Stereographic projections of EF_3 recumbent fold hinges.

Figure 3.2b: Stereographic projections of BF_2 folds. Note comparison of lineation orientations within these folds and steep zones.

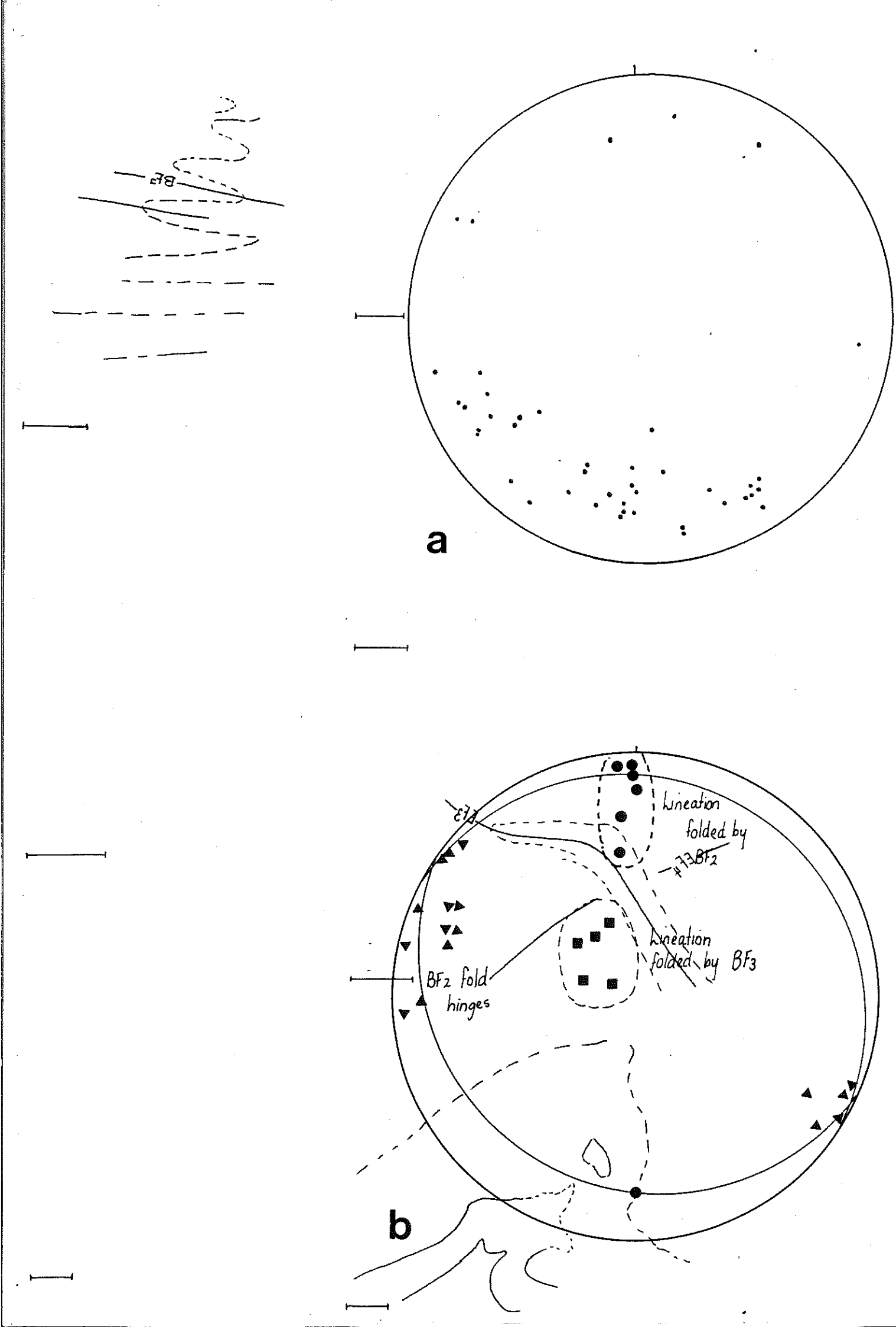
a
b
Lineation folded by F3BF2
Lineation folded by BF3
BF2 fold hinges

Figure 3.3: Field sketches.

(a) Fold hinges in layered amphibolite showing weak development of axial planar fabric (aligned hornblende grains) in EF_1 folds. Scale is 10cm.
(b) Dextral faulting of 'quartzite' within the Layered amphibolite map unit. Note warping of the enclosing amphibolite layering above the faults.
(c) BF_2 fold within the Granitic gneiss illustrating shearing parallel to one limb.
(d) Rotated layered amphibolite boudin within the biotite garnet schist of the Irindina supracrustal assemblage.

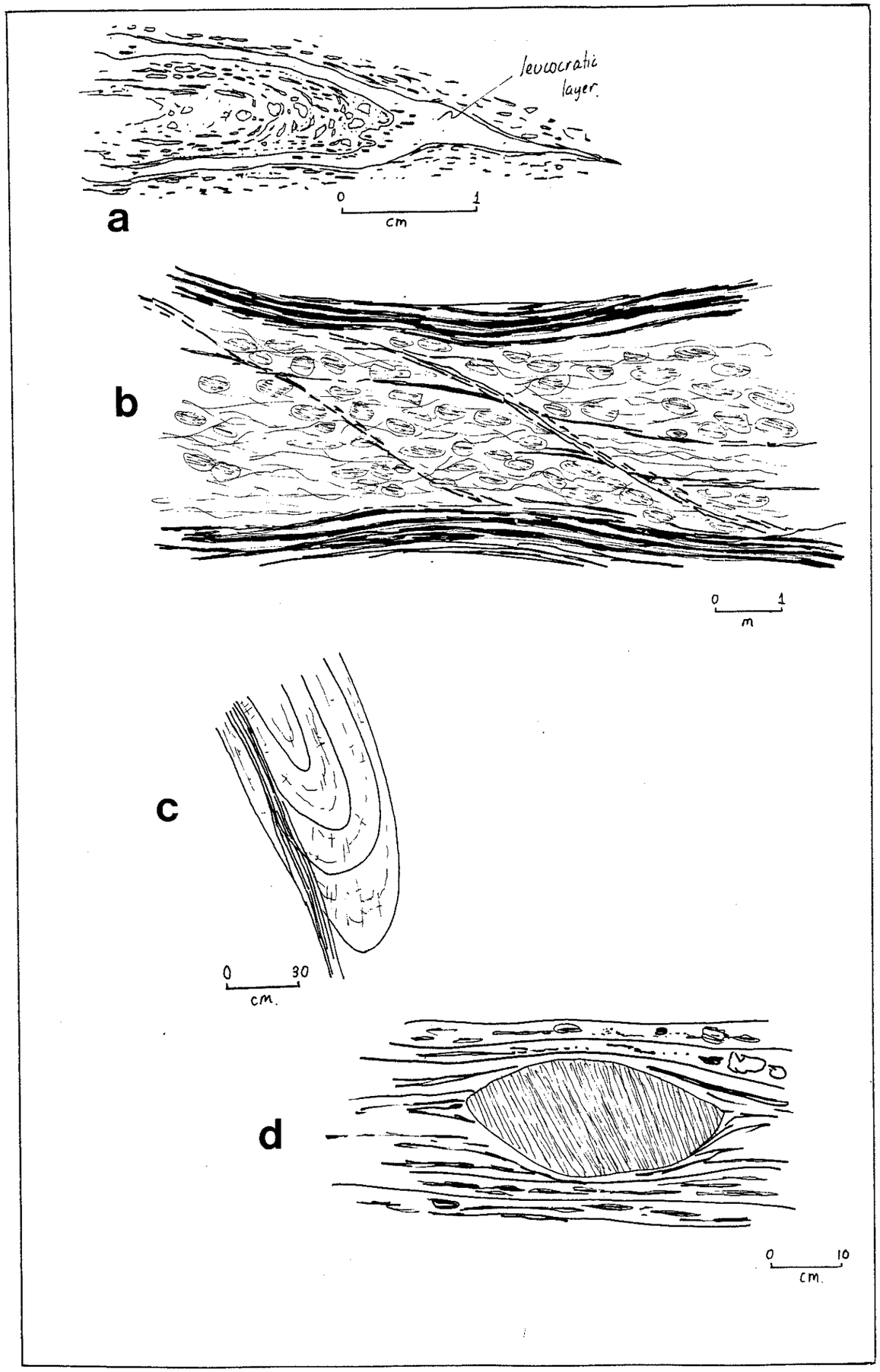

Figure 3.4: 'Anatomy' of BF_3 (steep zones).

(a) Detailed form map of locality number 97 illustrating folding of BS_2 foliation and lineation around an almost recumbent BF_3 fold hinge. Note change of vergence of lineation/foliation. BF_3 trends toward 079deg.
(b) Stereographic projection of data shown in (a).
(c) Detailed form map of locality number 99 illustrating the warping of BF_3 fold hinges by ED_4.
(d) Simplified sketch illustrating the style of the BF_3 folds.
(e) Stereographic projection of BF_3 fold hinges indicating effects of subsequent BD_4. Note the change in orientation from predominantly E-W, horizontal hinges to N-E and N-W slightly inclined orientations.
(f) Simplified sketch illustrating the warping of BF_3 folds by BD_4 deformation.

Figure 3.4

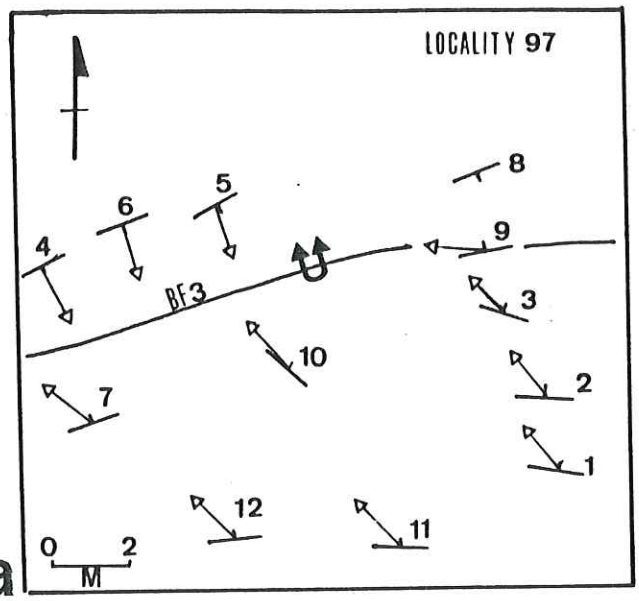

a

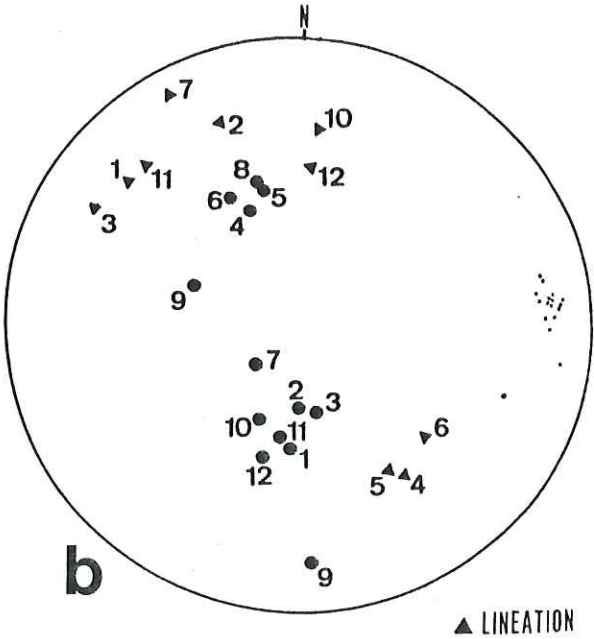

b

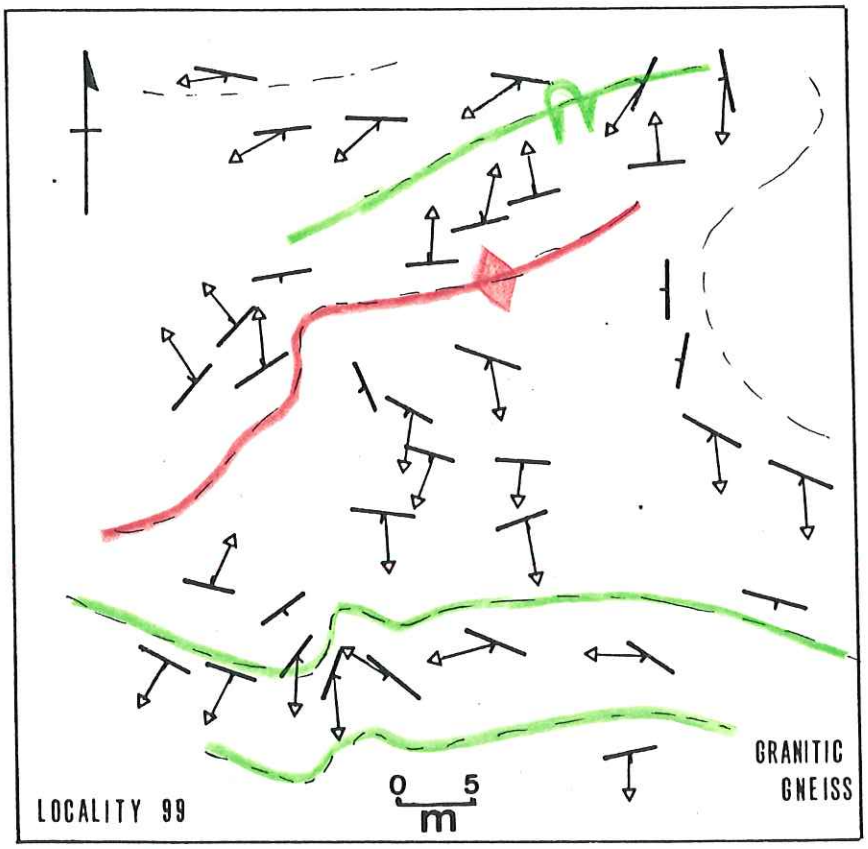

c

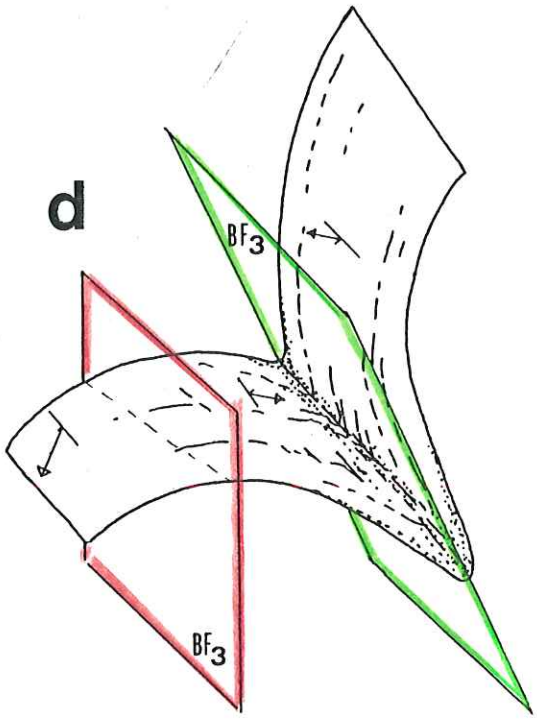

d

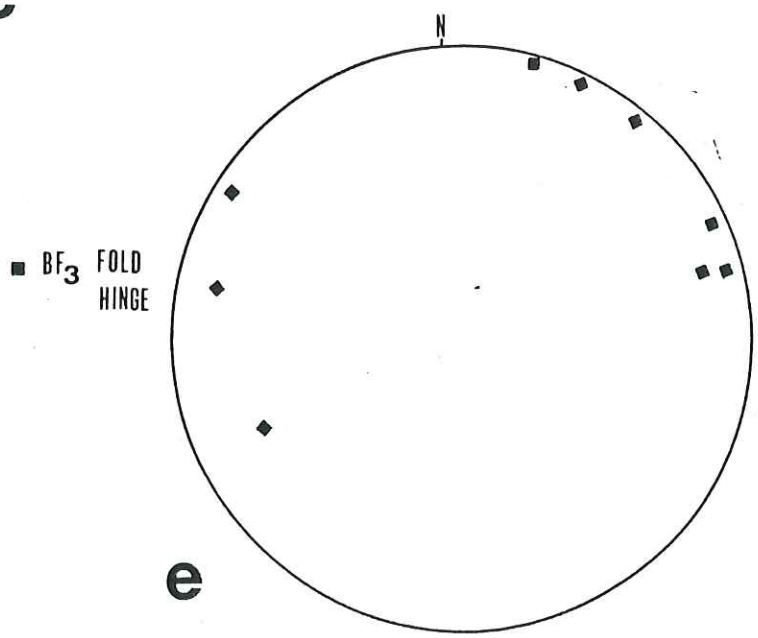

e

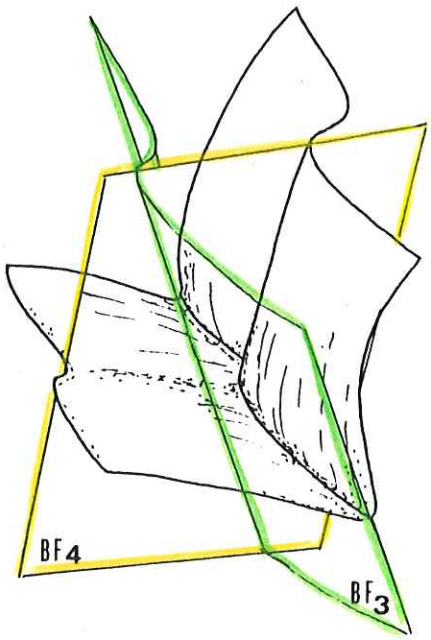

f

Figure 3.5: Maps of lineation trends and contoured foliation dips.

(a) Summary of lineations mapped throughout the study area. Note their general orientation is perpendicular to both upper and lower contacts of the Bruna gneiss, except where steeply plunging to the west due to BF_3 folds.
(b) Contoured map of the regional gneissic layering (ES_2, BS_2, IS_2) highlighting the steep zones within the Bruna gneiss.

Figure 3.6

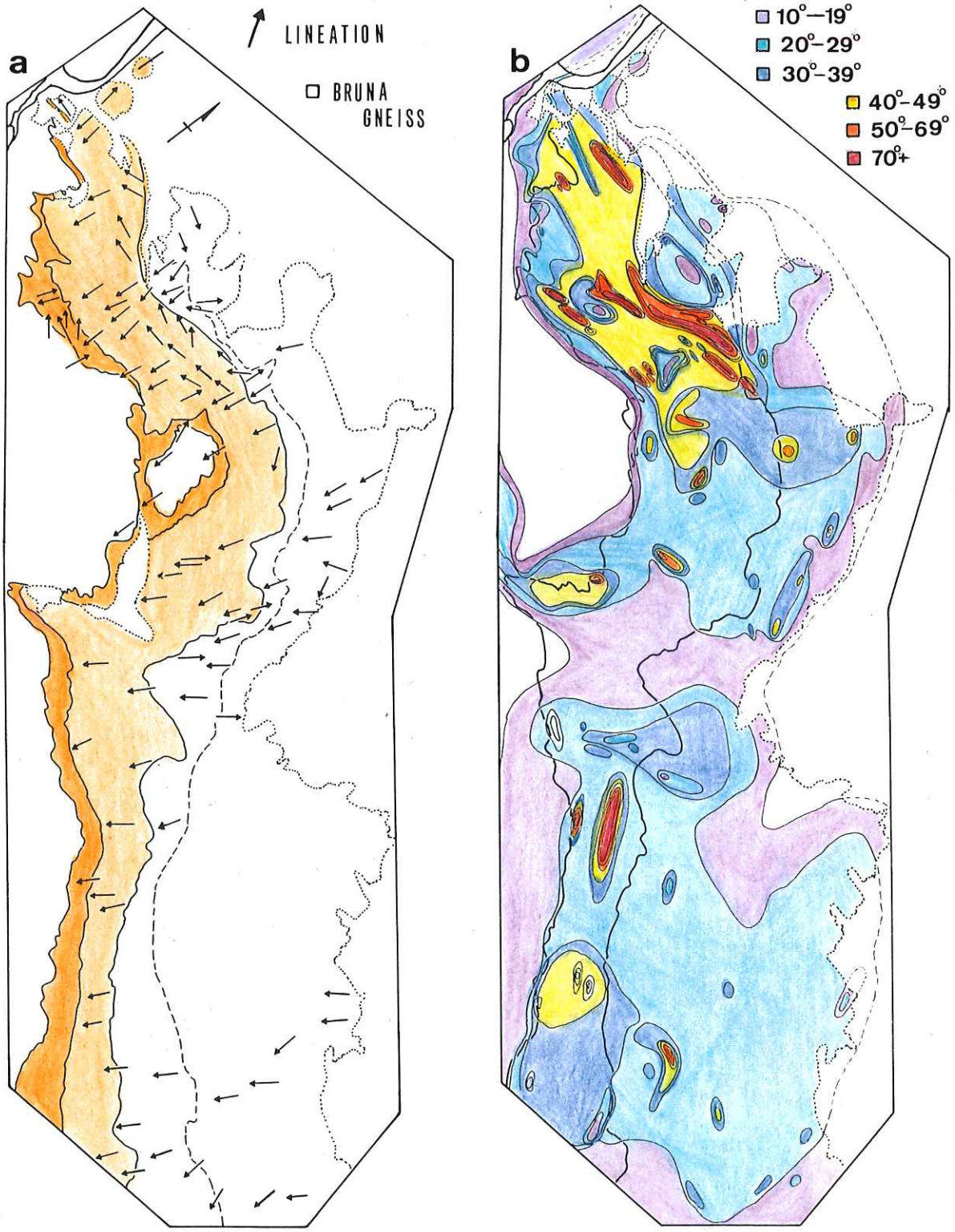

Plate 9: Layered amphibolite within the Migmatite map unit. Note the isoclinal EF_1 folds partially transposed, and the low angle discordance between internal layering and the gneiss/amphibolite contact. (Scale is 10*cm*.)

Plate 10: Granitic gneiss with 'stacked' BF_2 recumbent folds. (Scale is 30*cm*.)

Plate 11: Elongate, mafic boudins with hook-like terminations and flame structures with migmatitic gneiss. Note the thin (white) quartzose segregations initiated at the tips of the mafic stringers. (Scale is 30*cm*.)

Plate 12: Vertical layers in the flexure of the EF_4 asymmetric folds. Layer parallel compression has buckled the boudin/lens of the leucocratic gneiss. The horizontal 'fractures' are narrow parallel zones of recrystallized biotite. (Scale is 30*cm*).

Plate 13: Asymmetric EF_4 fold flexure refolding an isoclinal EF_3 hinge within the Migmatite map unit. (Scale is 30*cm*.)

Plate 14: Pale green epidote rich calc-silicate boudins rotated within the closure of an asymmetric EF_4 fold. (Scale is 10*cm*.)

Plate 15: Disharmonic folding and boudinage of migmatic gneisses and layered amphibolite around the hinge of an inclined EF_3 fold. Note box fold within layered amphibolite. (Scale is 30*cm*.)

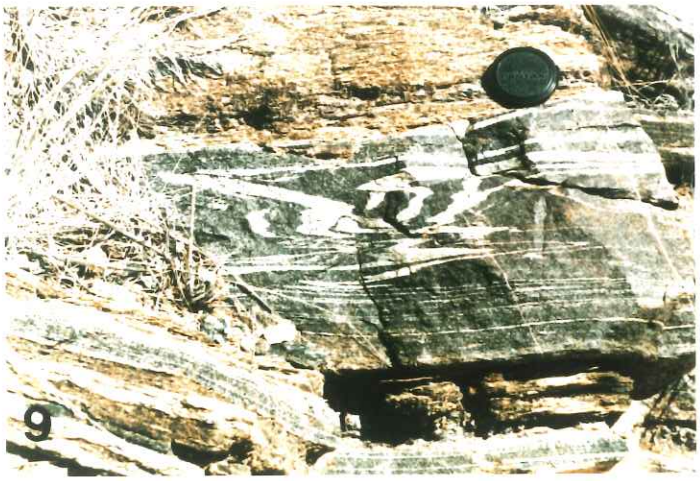
9


11


12


13


14


15

Plate 16: Mesoscopic , asymmetric EF_4 fold within the Layered amphibolite map unit. (Scale is $1m$.)

Plate 17: Horizontal, isoclinal, angular EF_3 fold warped by ED_5 deformation. Note the open dome crosscut by parallel veins. (Scale is $1m$.)

Plate 18: Small scale, intrafolial, isoclinal BF_1 folds in the Granitic gneiss. Note the elongate augen axial planar to the folds. (Scale is $10cm$.)

Plate 19: Numerous ptygmatic folds in a quartzofeldspathic segregation around an isoclinal BF_2 fold within the Granitic gneiss. (Scale is $30cm$.)

Plate 20: 'Steep zone' of gneissic banding (of the Granitic gneiss) within the hinge of a BF_3 fold. (Scale is $30cm$.)

Plate 21: Isoclinal, recumbent BF_2 fold of the contact between the Granitic and Megacrystic gneisses. (Scale is $1m$.)

Plate 22: Strongly developed lineation of the Megacrystic gneiss defined by elongate feldspathic augen, hornblende grains and quartz ribbons. XY section, lineation plunging south. (Scale is $10cm$.)

Plate 23: Mafic schlieren and attenuated megacrysts within the amphibole rich, streaky grey sublithology of the Granitic gneiss. This rock type occurs close to the contact with the structually overlying Megacrystic gneiss. (Scale is $10cm$.)


16


17


18


19


20


21

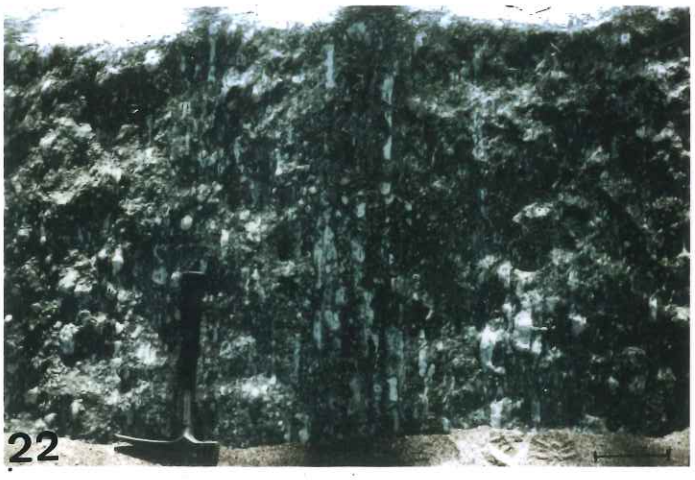
22


23

Chapter 4
Microfabrics

4.1 Introduction

Previous investigations within the Harts Range region describe the development of high grade tectonothermal fabrics and mylonites associated with complex ductile and semi-ductile deformation events (James et al., 1985; Rankin & James, 1984). The aim of this descriptive microstructural analysis is to:

- Identify any microstructural evidence of strain and movement.
- Establish some relative time sequence for the development of the microfabric elements and correlate this with mesoscopic observations.

Thin sections prepared for this study were cut parallel to the tectonic XZ and YZ sections, the X direction defined by the dominant lineation and the XY section parallel to the foliation (and principal plane of flattening strain).

4.2 Microstructures of the Entia gneiss lithologies

The microstructures and fabrics of the Entia gneiss lithologies are essentially related to the main, high grade tectonothermal event ED_2, with variable modification and overprinting of these fabrics produced during subsequent deformations.

4.3 Microstructures of ED_2

This peak metamorphic event produced the equigranular to elongate granoblastic textures within the quartzofeldspathic gneisses, with coarse grained biotite laths evenly distributed and strongly aligned throughout the matrix.

Within the compositional banding of the amphibolites and calc-silicates, the constituent ferro-magnesian phases typically have a strong shape preferred orientation parallel to ES_2. Parallel, elongate hornblende rhombs typically define the lineation, and small, secondary grains tend to be slightly elongate along the host grain cleavages. The felsic minerals tend to be more equant grains forming as aggregates within elongate augen or ribbons (although they are typically elongate where they coexist with amphibole).

The granoblastic, polygonal plagioclase grains are generally strain free and often untwinned, or have a single twin plane that bisects a triple point grain boundary junction. The grain margins are straight to gently curving and there is very minor triangular shaped subgrain development adjacent to triple points (see plate

24). Larger, irregular plagioclase grains occur in the coarse, elongate aggregates scattered throughout most layered amphibolites. These grains are strongly strain shadowed, with lobate to serrate boundaries, with small new grains scattered along the boundaries. This has been described as 'protoclastic texture' by Brown et al (1980). The marked recovery structures in the larger plagioclase grains indicate deformation has occurred above the disordering temperatures of plagioclase (approximately 550°) (White, 1976; Alm et al., 1980). Strain free polygonal plagioclase is often interpreted as having formed during post tectonic annealing (Sodre Borges & White, 1980), however the coexistence of the two forms of plagioclase suggests the polygonal texture has formed from the dynamic recrystallisation of coarse plagioclase during the upper amphibolite tectonothermal event.

Quartz sheets are extremely well developed in the calc-silicates (plate 34). The regular (1mm) laminae are comprised of subrectangular, elongate quartz grains; each grain occupying the entire width of the ribbon or sheet. The quartz-quartz boundaries within the ribbons are straight to gently curved and perpendicular to the length of the layer. Grains of similar length tend to have the same optical orientation (as shown by the tint plate) and are sometimes adjacent to each other. These 'associations' of 2-5 large grains are spaced by narrower, quartz grains with irregular grain boundaries and differing optical orientations. The quartz grains show internal strain with undulose and patchy extinction and subgrain development adjacent to grain boundaries.

The smooth quartz-quartz boundaries and their consistent alignment perpendicular to the laminae are believed to have formed during secondary recrystallisation after formation of the quartz ribbons (Culshaw & Fyson, 1984; Burg, 1986). It appears that some grains, suitably oriented for a faster growth rate parallel to the quartz sheet, have grown at the expense of unfavourably oriented grains. This explains the relationship observed between large grains and similar optic orientations. Evidence of grain growth is indicated by the greater grain boundary irregularity between quartz grains of different optical orientation. This growth is interpreted to have occurred late in ED_2. The internal strain features appear to be related to a later deformation.

4.4 Microstructures of Post-ED_2 Deformations

Evidence of shearing, producing proto- and blasto-mylonites occurs throughout the Lineated Leucocratic gneiss map unit. Augen bearing layers of the felsic gneiss contain asymmetric, partially recrystallised feldspar megacrysts wrapped by quartz ribbons. A well developed lineation is typically associated with the tectonites. Coarse grained quartzites display dislocation creep deformation, with quartz grains displaying intense deformation banding, subgrains and finely lobate grain boundaries, and subgrain development.

The formation of these L-S tectonites may be related to shear stresses associated

with EF_3 or EF_4 folding (Rankin, 1983; Martin, 1983). However, the proximity of this map unit to the Bruna gneiss and its persistent, southerly trending lineation (parallel to lineations within the Bruna gneiss) suggest discreet mylonitic zones developed within the Entia gneiss complex during juxtaposition of the 'cover' with the 'basement'.

At the microscopic scale, incipient overprinting involving axial planar recrystallisation of biotite occurs within EF_3 fold hinges. This fabric was not observed away from the fold closures or at the hand specimen scale.

The ultramafic intrusive (see section 2.2.8) is massive to weakly foliated. The olivine-clinopyroxene meta peridotite is cut by numerous parallel fractures that increase in density as they penetrate the olivine phenocrysts. There is no offset along them, however replacement by extremely fine material along the fractures and lamellae produces a fine 'train track' texture. Kink bands, slightly mis-orienting the clinopyroxene lamellae, are the sites of recrystallisation.

The meta-hornblendite appears to formed by complete replacement of pyroxene by hornblende. The fine amphibole grains are inequigranular, semi-randomly oriented, with the outlines of old kink bands recognisable. Sericitised plagioclase augen in the hornblendites are elongate and define a weak foliation. The augen consist of polygonal, equigranular plagioclase with gently curved grain boundaries and triple point junctions. The weak development of the foliation does not increase simply from core to mantle of the elliptical intrusive, suggesting mineralogical control on its development was predominant over the effect of external stress fields.

The metamorphosed ultramafic intrusive is believed to have intruded the basement lithologies at some stage following the peak metamorphism ED_2 but before major shearing associated with the Bruna gneiss.

4.5 Microstructures of the Bruna gneiss

Both the Granitic and Megacrystic gneisses clearly display microstructural evidence of shearing and grain size reduction, predominantly by ductile deformation (recovery and recrystallisation) and rarely by brittle fracture. Some aspects of the microstructural development are summarised here (for more detailed descriptions see Appendix I).

The granitic and megacrystic gneisses that comprise the Bruna gneiss have been previously described as L-S tectonites, in particular as 'blastomylonites' (see Martin, 1983; Rankin, 1983; Ding et al, 1983). Following the terminology of Bell and Etheridge (1973) a mylonite is a "foliated rock, commonly lineated and containing megacrysts, which occurs in narrow, planar zones of intense deformation". White (1982) after Sibson (1977) has proposed a classification of mylonites based on general grain size reduction (gradational from parent material) and the mechanisms

producing this refinement. White (1982) defines a 'blastomylonite' as having undergone up to 50% recrystallisation to fine matrix. The Bruna gneiss is believed to have intruded an active shear zone. This implies that the original material was not necessarily homogeneous nor undeformed, and it may not be correct to imply a degree of mylonitisation (Takagi, 1986). However, the feldspathic megacrysts within the Bruna gneiss and adjacent gneisses have been partially to completely replaced by finer grained recrystallised grains, and the mylonite terminology is still applicable. Comparison of these samples with those from other, well documented mylonitic rocks indicates the recrystallised matrix of the Bruna gneisses are generally more coarse grained than typical mylonites (Obee & White, 1985).

4.6 Microstructures Associated with BD_1

The L-S (or blastomylonitic) fabric of the gneisses developed during both the early deformation phase BD_1 (with the intrafolial BF_1 folds buckling an incipient fabric (BS_1)) and a more intense BS_2 foliation developing simultaneously axially planar to them. The BS_1 foliation can only be identified in the BF_1 fold hinges – it differs from BS_2 only by the finer grain size of the granoblastic, elongate quartzofeldspathic matrix. The BS_2 foliation (and lineation) defines the pervasive gneissic banding that has been mapped in figure 1.

Plagioclase and K-feldspar megacrysts in both gneisses have core and mantle structure (White, 1982), reflecting the strain gradient across the megacryst margins. Plagioclase megacrysts display bending, tapering and microcracking of polysynthetic twins and deformation twinning on the pericline law. The K-feldspar grains are more likely to display internal deformation banding that disrupts internal perthitic and microcline textures. The grain margins are finely embayed or serrate and mantled by a fine granoblastic equigranular to elongate mosaic of clear, commonly strain free feldspar, quartz and myrmekite, (plate 28). Recrystallised grains are equant and coarser grained on the 'sides' of the augen (*ie* the sides perpendicular to the XY plane).

The megacrysts of the granitic gneiss average only 1-2 cm diameter. The augen are either subrounded, single grains or flattened aggregates that are strongly sericitised (*cf* the megacrystic gneiss). The grey, streaky gneiss component contains extremely attenuated hornblende aggregates (xenoliths?) and quartz ribbons in layer parallel bands of variable feldspar, quartz and biotite content. The quartz ribbons are moderately strained, with deformation banding perpendicular to the ribbon. Very fine ($\approx 100 \mu m$) biotite laths parallel to the ribbon margins are included within the quartz grains. These inclusions indicate a much finer, oriented mica phase existed before growth of the quartz grains to form ribbons. The biotites are controlling the recrystallisation of the strained quartz, with the irregular subgrains and new grains forming adjacent to the mica (plate 26). Kinking of one muscovite grain was noted in the muscovite quartzite. The kink band boundaries

within the coarse, old mica grain are parallel to the elongate single laths that define the schistosity. It is possible that the muscovite has recrystallised from kink limbs that have been rotated into parallelism with the principle plane of flattening (Etheridge & Hobbs, 1974).

The large (5cm) feldspar augen in the megacrystic gneiss show a wider range of shapes and sizes. Some megacrysts are quite rounded in the the YZ section despite advanced recrystallisation (plate 33). The amount and coarseness of recrystallised matrix is also variable. This reflects the importance of crystallographic orientation on intragranular deformation and the extent to which the biotite rich matrix has preferentially deformed around the augen.

Garnet porphyroblasts are large and often subrounded in the Megacrystic gneiss (unlike the Granitic gneiss where the occasional garnet is extremely altered and attenuated). These porphyroblasts, with inclusion trails of lobate quartz and biotite are frequently bordered by distinctive pressure shadows (plate 29).

4.7 Microstructures of Post BD_1 Deformations

The finely crenulated hinge zones of rare BF2 folds exhibit faint axial planar development of lepidoblastic biotite. The crenulations are most clearly defined by tightly folded 0.5mm–2mm wide quartz ribbons, the margins of which are pinned by ragged, embayed green-brown biotite flakes. Strings of opaques, included by or adjacent to these 'old' biotite grains also clearly define the BS_2 foliation. New, finer grained, subidioblastic biotite sporadically occurs at a high angle to the quartz ribbon margins, defining the weak axial planar BS_2 fabric. The quartz ribbons have completely recrystallised into serriate, equant grains, decreasing in size in the crenulation hinges.

Discontinuous 'biotite stacks' that produce short compositional bands at an oblique angle to the BS_2 fabric are observed only within the Megacrystic gneiss. These structures, resembling the "spaced asymmetric crenulations" of Law et al (1984) may be analogous to the "cisaillement" ("c") planes of Berthé *et al* (1979), or shear surfaces of White et al (1980). The bands, at an angle of 16° to the BS_2, consist of biotite only – no grain size reduction or offset of layering is associated with them. They are discontinuous and indistinct, being confined to the biotite rich layers, and at these layer margins they merge into parallelism with the BS_2 fabric.

These structures may have developed as a consequence of coaxial flattening oblique to the BS_2 (forming an "extensional crenulation" (Simpson & Schmidt, 1983)), however only one set of surfaces occur, with their sense of 'shear' being consistent with asymmetric augen criteria (chapter 5). According to White et al (1980):

> "It is probable that in many instances the shear bands may represent the final phase of ductile deformation in a shear zone as the

temperature drops."

As the "shear bands" are only observed in the Megacrystic gneiss, it is not clear to which deformation phase they are related.

The Granitic and Megacrystic gneisses are clearly differentiated not only on the basis of mineralogy but on microstructural grounds as well. The granitic gneiss is overall a medium to fine grained granoblastic L-S tectonite, with penetrative compositional and grain size banding. The Megacrystic gneiss is also a L-S tectonite, but with megacrysts more variable in size, shape and composition. The size and subrounded shape of the garnets, the coarseness of strain free biotite in pressure shadows, less distinctive quartz ribbons and the less regular, lensing foliation indicate a different set of deformational conditions existed between the two units. This is discussed in Chapter 6.

There appears to be no microstructural development associated with BD_3 or subsequent folding.

4.8 Microstructures of the Irindina supracrustal assemblage

The biotite garnet schists of the Irindina supracrustal assemblage are poorly layered but strongly foliated, the green/pale-yellow biotite forming anastomosing, thick decussate aggregates and strings around elongate quartz and feldspar grains. There is evidence that both plastic and brittle deformation has occurred, with plagioclase megacrysts displaying fractured albite twins, and quartz ribbons exhibiting deformation banding perpendicular to their length. Garnet porphyroblasts have been fractured and pulled apart, with coarse biotite infilling the spaces. These microstructures appear to be related to ductile shearing that accompanied the overthrusting of this 'cover' sequence, as spaced asymmetric crenulations (discussed previously) occur in some biotite rich bands (plate 32).

Fine grained 'mylonites' occur in thin (10cm) layers close to the lower contact of the Irindina assemblage. These consist of alternating plagioclase- and K-feldspar-quartz-garnet bands. Asymmetric feldspar aggregate spindles are strongly parallel to quartz sheets that encompass strung out, embayed garnets (plate 31). It is interesting to note the absence of oblique fabrics in these biotite poor layers.

The megacrystic gneiss near the base of the Irindina supracrustals clearly indicates shear deformation occurred in the 'cover' sequence. The discontinuous megacrystic unit can be seen to grade from a very coarse grained 'protomylonite' where large (10cm) feldspar fragments are cut by anastomosing fractures to a 'blastomylonite' of subrectangular to subrounded, partially recrystallised asymmetric augen in a schistose matrix. The strong resemblance between this lithology and the Megacrystic gneiss of the Bruna gneiss is significant although the two are invari-

ably separated by layered amphibolite. According to Vernon (1986), K-feldspar megacrysts only originate from igneous accumulations, and do not grow as porphyroblasts. Therefore the megacrystic gneiss within the Irindina supracrustals may be part of the protolith of the 'Bruna' Megacystic gneiss that intruded the cover sequence, see (Ding & James, 1985; James & Ding, in press).

Photomicrographs

The following key is applicable to all photomicrograph plates:

K = K-feldspar
q = quartz
P = plagioclase
g = garnet
b = biotite
a = hornblende
e = epidote
o = olivine
m = myrmekite
s = scapolite

All have crossed nicols, except plates 30, 31 and 32.

(Scale bar $1mm$)

Plate 24: Photomicrograph of recystallised plagioclase within a weakly foliated layered amphibolite. Note the inequiangled triple point junctions between the polygonal, strain free, rarely twinned plagioclase grains. Hornblende shape preferred orientation defines the ES_1/S_2 fabric, parallel to the long axis of the plate. Sample (865-50).

Plate 25: Photomicrograph of finely recrystallised plagioclase(?)/clinopyroxene(?) matrix and partially pseudomorphed plagioclase in meta-peridote. Note the 'fringe' of feathery grains perpendicular to the ragged plagioclase grain, and the high density of fractures penetrating the olivine grains. Sample (865-22).

Plate 26: Photomicrograph of Megacrystic gneiss, the irregular quartz ribbon partially recrystallised to smaller, new grains. Note the fine, oriented biotite inclusions controlling subgrain development. Lepidoblastic biotite defines the BS_2 foliation. Sample (865-67 XZ).

Plate 27: K-feldspar, strain shadowed megacrysts within the Megacrystic gneiss. Note the polycrystalline, finely recrystallised margins that include myrmekite, hornblende, granoblastic K-feldspar, quartz and biotite. Sample (865-68 YZ).

Plate 28: K-feldspar megacryst with marginal recrystallisation to very fine new grains. Note the quartz filled fracture with well developed deformation banding indicating the quartz has plastically deformed more readily than the K-feldspar. Megacrystic gneiss (865-68 XZ).

Plate 29: Garnet porphyroblast within the Megacrystic gneiss. Note the fine grained quartz hornblended, feldspar and biotite inclusions within the marginal zone indicating a late stage of porphyroblast growth that incorporated the recrystallised matrix. Subidioblastic epidote appears to be in equilibrium with coarse grained brown-green biotite. Sample (865-68 XZ).

Plate 30: Poikiloblastic garnet, elongate parallel to IS_2 is rimmed by coarse grained decussate, green biotite. Note the aligned inclusions of green biotite and quartz parallel to IS_2, indicating the garnet developed syn-ID_2. Sample (865-55).

Plate 31: Stained thin section of the felsic mylonitic gneiss within the Irindina supracrustal assemblage. The plagioclase aggregates are stained red, K-feldspar grains and biotite appear black. Note the asymmetric retort shape of the plagioclase and embayed garnet. Sample (865-54 XZ).

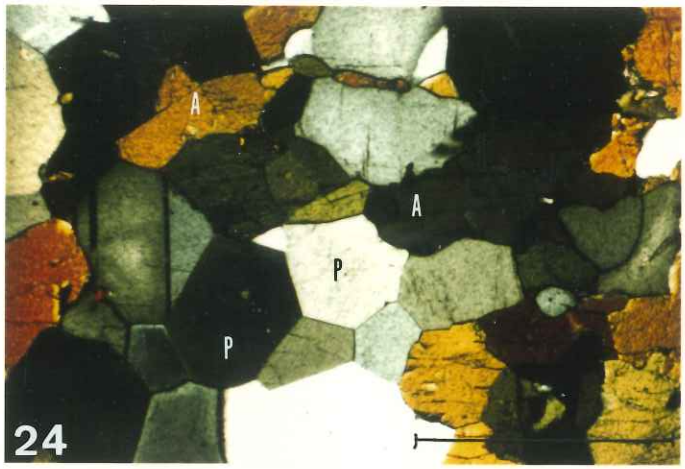
A
A
P
P
24


O
P
O
25

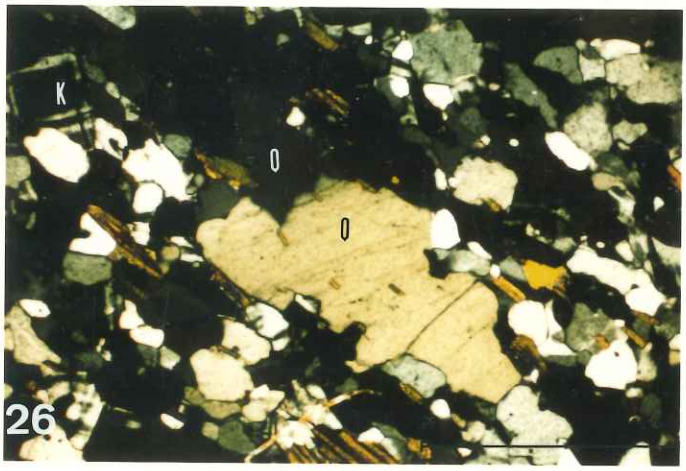
K
O
O
26


K
M
K
27

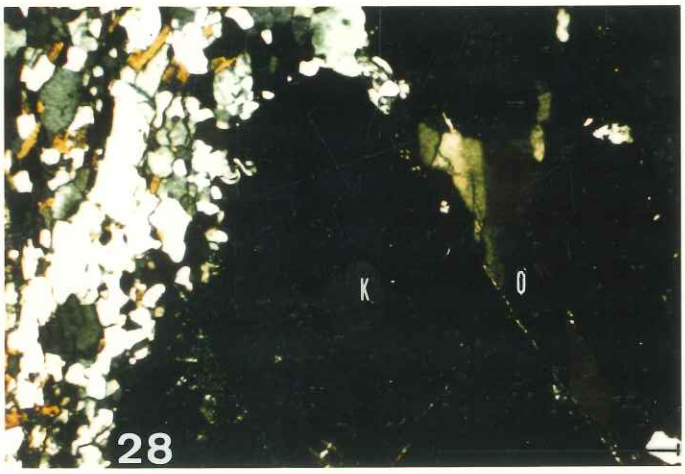
K
O
28

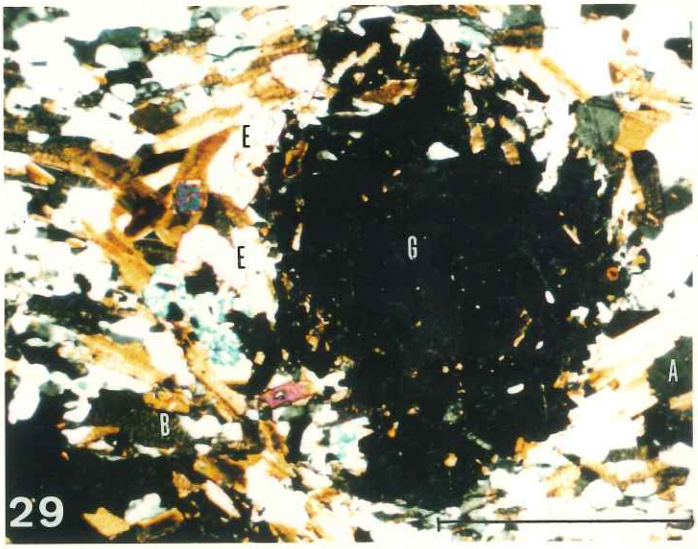
E
E
G
A
B
29

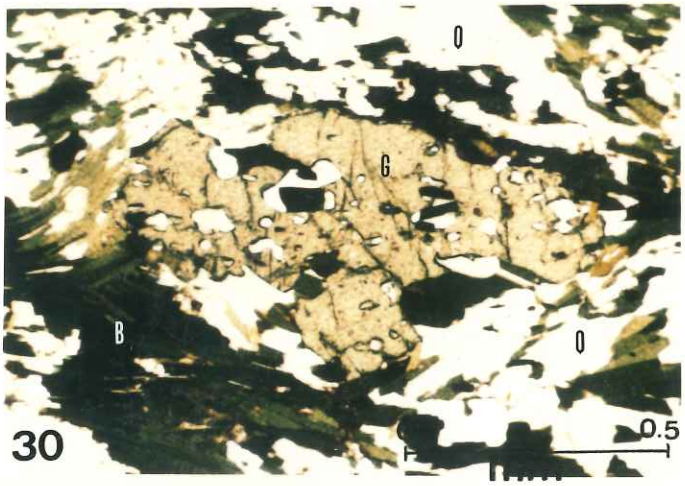
O
G
B
O
0.5
30


P
P
G
O
G
O
K
0
0.5
mm
31

Plate 32: Spaced asymmetric crenulations within a megacrystic lens of the biotite-garnet schist; 'Irindina' supracrustals. The compositional layering, parallel to the long side of the photomicrograph, is disrupted by low angle, indistinct surfaces. Whole this section photographed. Sample (865-55).

Plate 33: Megacrystic gneiss YZ section illustrating subrounded, partially recrystallised K-feldspar megacrysts set in a biotite-rich, fine grained granoblastic elongate matrix. Whole this section photographed. Sample (865-68 YZ).

Plate 34: Photomicrograph of deformation banding within quartz laminae of a calc-silicate (Entia gneiss complex). Note strong shape preferred orientation of epidote, hornblende and scapolite, parallel to the quartz sheets. Sample (865-80).

0 0.5 mm

0 0.5 mm

32

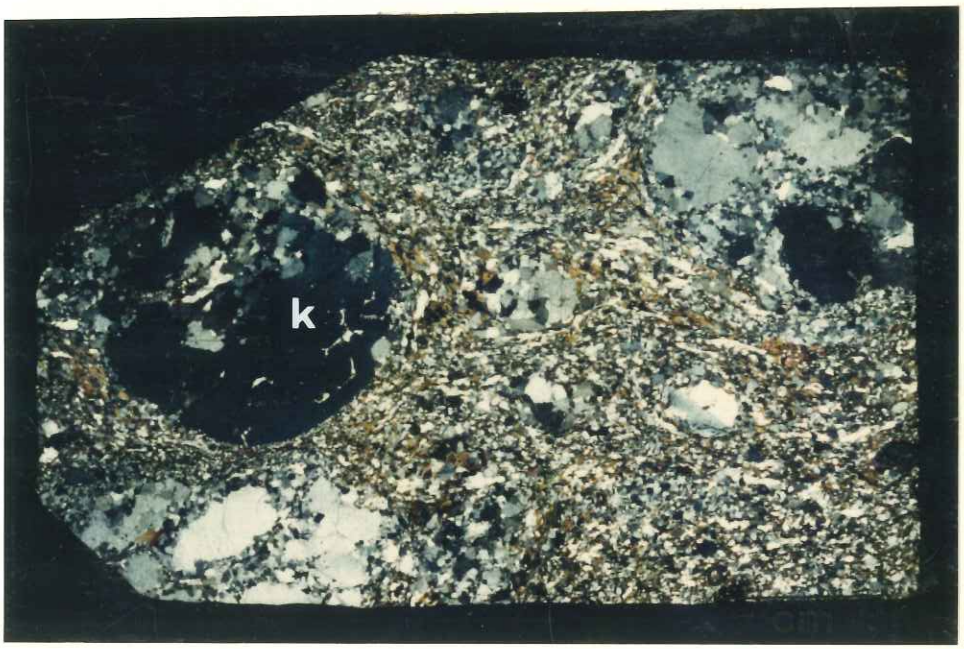

33

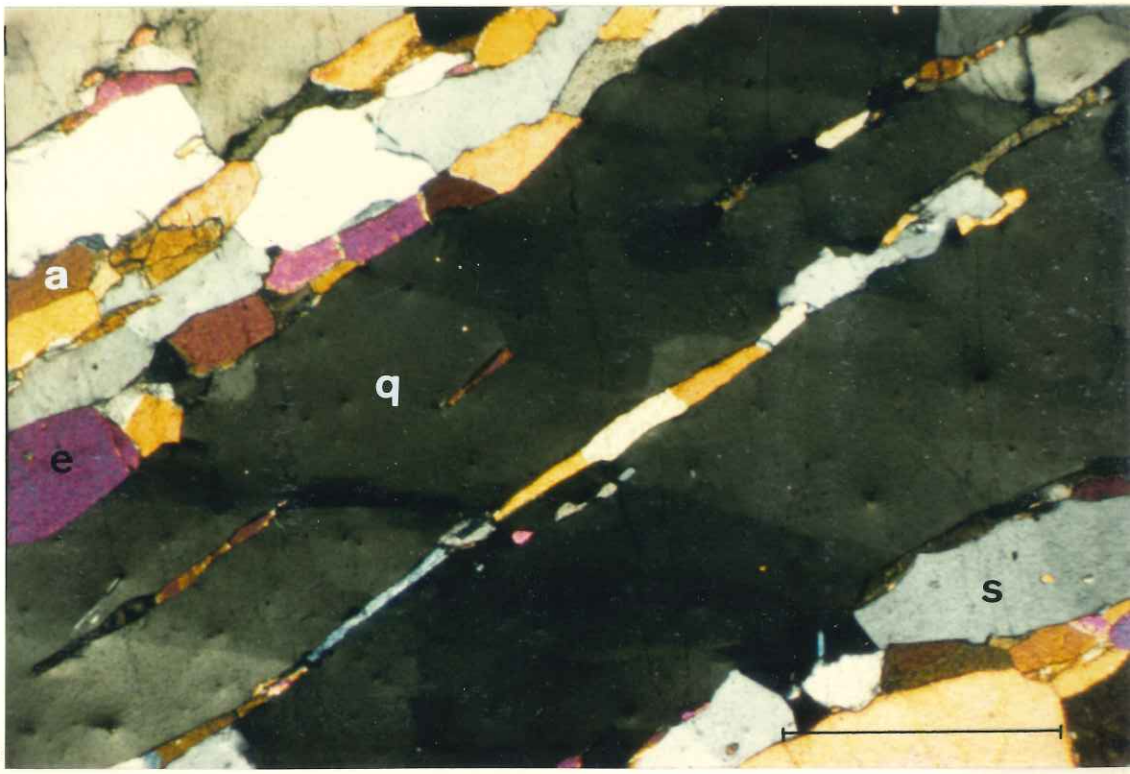

34

Chapter 5
Strain and Kinematic Analysis

5.1 Introduction

The development of high grade L-S tectonites with microstructural evidence of grainsize reduction through syntectonic recovery and recrystallisation indicates the Megacrystic and Granitic lithologies of the Bruna gneiss, and adjacent rocks occupy a zone of relatively intense deformation. Strain and kinematic analyses have been applied to these rocks in order to determine the nature and development of this zone.

5.2 Movement Direction

Lineations in the Bruna gneiss are defined by mineral and aggregate shape preferred orientations and correspond to the X principal strain axis. The lineation map of figure 3.6a can be used as a kinematic trajectories map (Teysier, 1985) indicating the direction of shearing associated with the formation of the L-S fabric (Brunel, 1986). The movement direction (indicated by lineations un-affected by significant folding) trends 350° to 020° (magnetic north, rotated to horizontal). This study agrees with other investigations in a broadly N/S thrusting direction of cover over 'basement' (Ding & James, 1985).

5.3 Sense of Shear

Asymmetric augen and pressure shadows were analysed to determine the sense of shear (Simpson & Schmidt, 1983) in twelve samples of the Granitic and Megacrystic gneiss and a mylonitic felsic gneiss within the 'cover' sequence.

Where a high ductility contrast occurs between a megacryst and its matrix, simple shear deformation will rotate the finer grained, and therefore weaker (White et al., 1980) tails into parallelism with the foliation. The coarser grained cores of the augen remain oriented obliquely to the tails allowing the sense of the megacryst rotation and hence the shear sense to be determined (Simpson & Schmidt, 1983). Feldspar megacrysts that have undergone little or no dynamic recrystallisation tend to give ambiguous results, therefore asymmetric, biotite + quartz filled pressure shadows around garnet porphyroblasts were used as a check on this analysis.

The feldspar augen typically have a symmetrical to retort shape, with tails of finer grained recrystallised material smeared out along the foliation. The asymmetry is observed in the XZ section indicating rotation around an axis parallel to the Y

principal strain axis, which also supports the use of lineation as a shear direction indicator. As shown in table II, both senses of shear were recorded within each sample, with one sense of shear usually predominant. Within the upper part of the Granitic gneiss, and the mylonitic gneiss of the 'cover' sequence, the asymmetry indicates a northward movement of an overlying layer, relative to the sample (figure 5.1). The opposite sense of shear (i.e. southwards) was observed in the Megacrystic gneiss. Ding and James (1985) suggest the Irindina supracrustal assemblage was overthrust in a southerly direction relative to its basement, however in this study only the microstructures within the Megacrystic gneiss indicate this southward overthrusting.

5.4 Strain Analysis

Three dimensional strain analysis via direct measurement of ellipsoidal megacrysts was carried out on seven samples from the Megacrystic, Granitic, Lineated Leucocratic and 'cover' mylonitic gneisses (figure 5.2a). Low to high strains were recorded, with the Granitic gneiss recording the highest strains (d=1.3, (Ramsay & Huber, 1983)). Within the Granitic gneiss, the megacrysts indicated pure oblate flattening with strain symmetry (Flinn k) values close to zero, the strain intensity increasing towards its upper boundary with the Megacrystic gneiss. The felsic mylonite of the 'cover' and the Megacrystic gneiss samples indicate higher strains, with strain symmetry values of 0.38–0.53 suggesting that deformation (at the scale of the hand specimen) consisted of a combination (*ie* 'transpression') two components: simple shear and limited pure shear (Berthe et al., 1979). An augen bearing lithology within the lineated Leucocratic gneiss indicated moderate intensity plane symmetry with k = 1.15.

In three samples, the individual megacryst types were differentiated and recorded separately on a Flinn plot (figure 5.2b) in order to analyse the relationship between the megacryst mineralogy and deformation. This graph clearly illustrates that the final strain configuration within any tectonite varies according to megacryst composition, crystallographic orientation and initial shape ratio, as well as to the rate and type of deformation.

The hornblende megacrysts in all three samples recorded high strains as expected from the typical undeformed amphibole shape prism shape. From the two samples of the megacrystic gneiss (one sample indicating a higher strain than the other from an adjacent layer) the recrystallised aggregates maintain similar k-values with increasing strains (figure 5.2b). The single grain and marginally recrystallised megacrysts changed shape, probably due to both their initial crystallographic orientation (relative to the principal strain axis), and degree of recrystallisation. This has important implications for the application of strain analysis to heterogeneous, highly strained rocks and emphasises that care should be taken over the type of ellipsoidal objects that are measured (Watts & Williams, 1983).

5.5 Discussion

A recent study of the Moine Thrust region by Law et al (1984) relates strain intensity and symmetry to position of the rocks within the Arnaboll and Upper Arnaboll Thrust Sheets. They correlate high, non-coaxial strains with proximity to the thrust surfaces, the middle to upper levels of the thrust sheet displaying lower intensity, coaxial strains. Following their interpretations the Megacrystic gneiss appears to have been more closely associated with thrusting of the 'cover' lithologies over the 'basement', the southwards sense of shear being clearly illustrated by the high ductility contrast occurring within this relatively biotite rich, large augen bearing lithology. The reverse sense of shear and the pure oblate strains recorded in the Granitic gneiss appear to be associated with the structural complexity and heterogeneous mineralogy within this unit. Recumbent, isoclinal folding of its upper contact and foliation within the Granitic gneiss indicates a significant amount of flattening perpendicular to the layering has occurred. This bulk flattening must have produced the oblate strains as well as the reverse sense of shear, as the inverted limbs (of recumbent folds unidentifiable without suitable exposure) must display the opposite shear sense to the normal limbs.

It is also possible that the mineralogy of the Granitic gneiss has affected its response to simple shear stress. This lithology, relative to the Megacrystic unit, has less contrast in grainsize, with smaller megacrysts that are partially to wholly recrystallised and set in a medium grained, biotite-poor, granoblastic matrix. The augen may have responded to the component of pure shear during ductile deformation (Berthe et al., 1979), being less able to deform non-coaxially due to the low ductility contrast between augen and matrix.

It is concluded that whilst bulk deformation of the Megacrystic gneiss approximates simple shear, deformation within the Granitic gneiss has involved both pure shear (flattening) and simple shear (rotation) components. The concentration of higher strain into narrow bands, notably at the top and bottom contacts, but also throughout the gneiss has been controlled mainly by its compositional heterogeneity and further complicated by internal recumbent folding. The variable mineralogy, rock textures and local deformation conditions at the thin section to outcrop scale have interacted to produce the interleaved, moderate to intense L-S fabric of the Granitic gneiss, whereas a simpler (therefore later?) deformation history is proposed for the Megacrystic gneiss.

Figure 5.1: Cartoon summarising sense of shear determination from asymmetric augen within the Granitic and Megacrystic gneisses, and the felsic mylonite of the Irindina supracrustals. Note the 'southward' movement direction indicated by the Megacrystic gneiss, and the reverse sense of shear within the other lithologies.

Figure 5.1

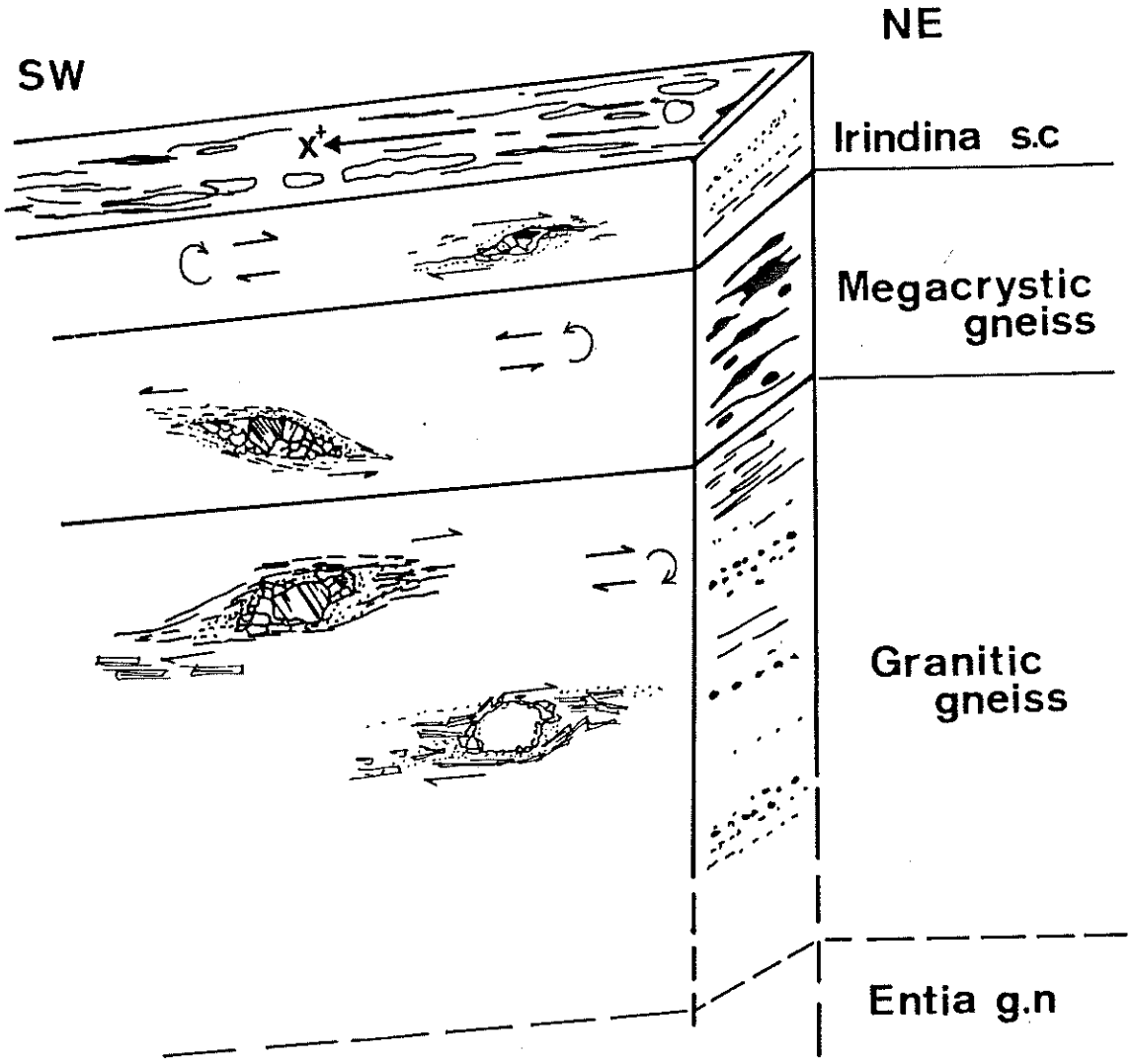
NE
SW
X+
Irindina s.c
Megacrystic gneiss
Granitic gneiss
Entia g.n

Figure 5.2: Flinn plots.

(a) Flinn plot of seven samples.
865-67 Megacrystic gneiss k=0.38
865-68 Megacrystic gneiss k=0.53
865-90 Granitic gneiss k=0.0
865-93 Granitic gneiss k=0.36
865-96 Granitic gneiss k=0.01
865-81 Lineated Leucocratic gneiss k=1.15
865-54 Irindina s.c. mylonite k=0.5

(b) Flinn plot of individual megacrysts types from three samples.

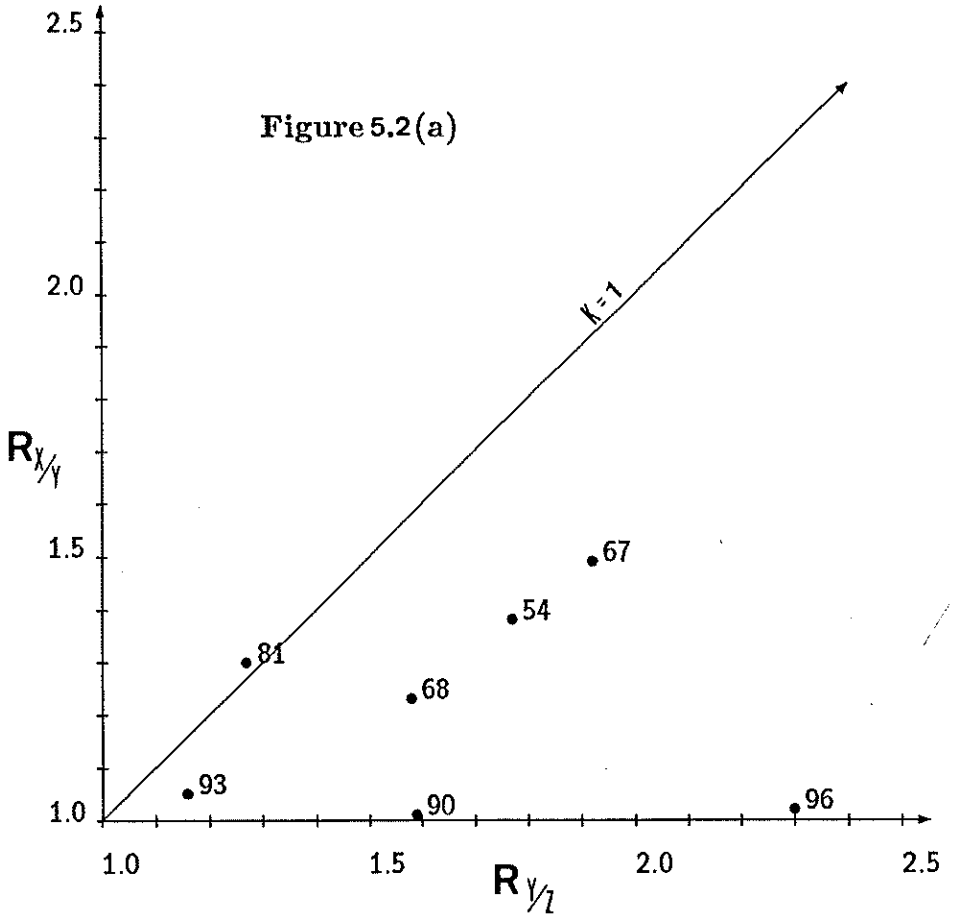

Figure 5.2(a)

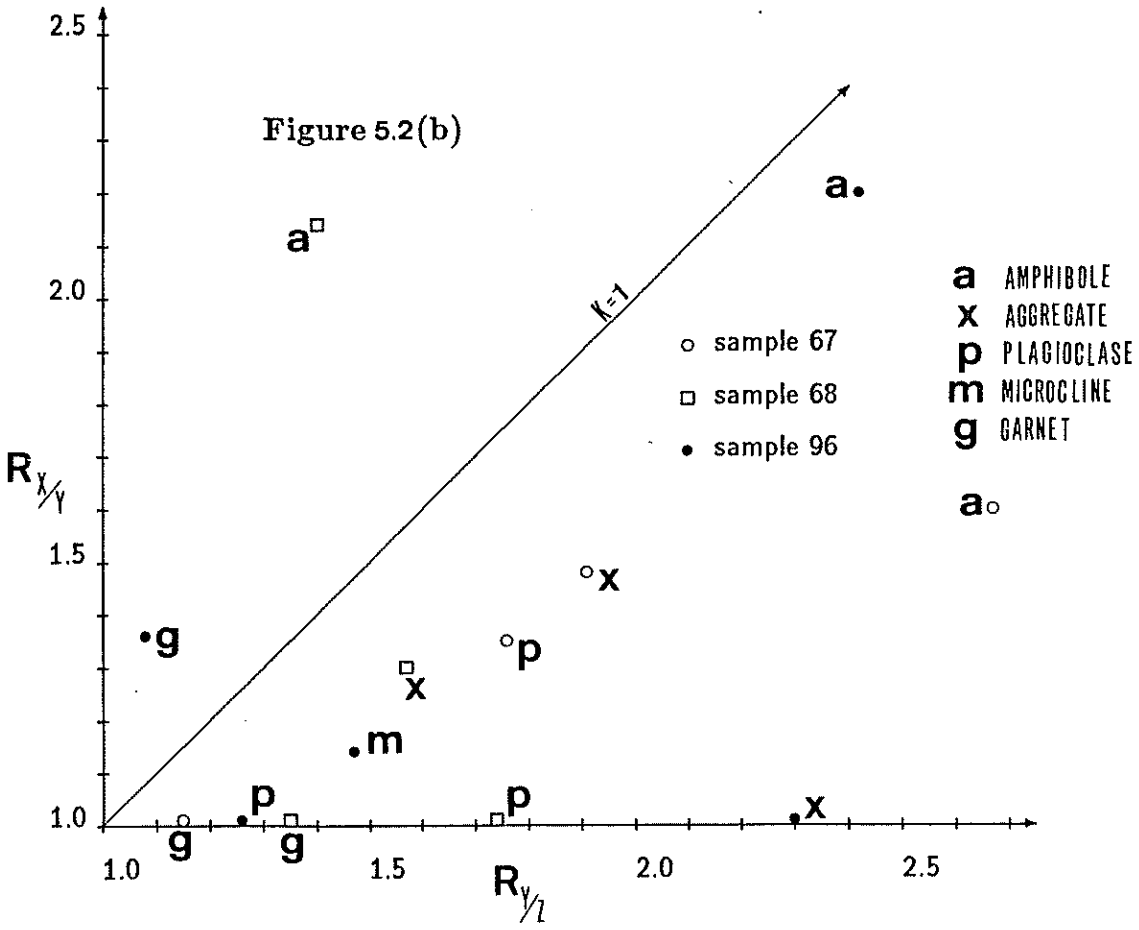

Figure 5.2(b)

	GRANITIC				MEGACRYSTIC					IRINDINA		
865-	70	9 H.S.	96 T.S.	94 T.S.	68 H.S.	68 T.S.	67 Ph	67 H.S.	67 T.S.	E Ph	54 T.S.(G)	54 T.S.(P)
	17.5	0	11.1	—	18.2	0	9	40	12.5	7	17.3	0
	25.0	25.8	29.	—	24.2	0	23	0	0	13	1.15	1
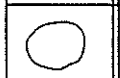	2.5	0	0	—	0	0	1	0	0	0	3.46	0
	47.5	32.2	33.3	—	24.2	13.6	35	43.3	0	51	43.3	41.2
	7.5	35.5	22.2	100	6.1	36.4	9	3.3	8.3	29	30.0	47.0
	0	6.4	3.7	0	27.3	50	24	13.3	79.2	0	4.6	10.6
n	40	31	27	3	33	22	101	30	24	41	173	85

Ph – Photograph H.S. – Hand Specimen T.S. – Thin Section G – Garnet Porphyroblasts P – Plagioclase/K-felspar

%

Table 2: Determination of sense of shear from asymmetric augen.

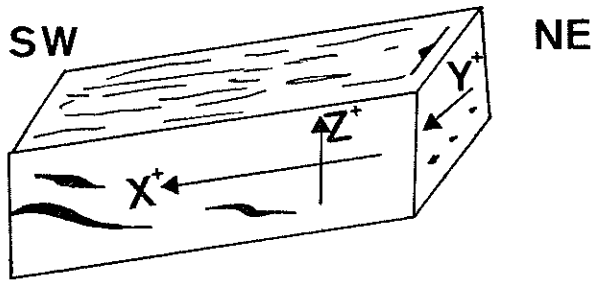

Chapter 6
Discussion and Tectonic Synthesis

The tectonic setting of orogenesis in the Early-Middle Proterozoic is a topic of considerable debate in the current literature. Although Etheridge et al (in prep) refer to one school of thought that is based on "the application of unmodified actualistic concepts of modern orogeny" to Precambrian tectonics, it is becoming clear that the majority of researchers prefer alternative models. Whilst acknowledging some geochemical affinities with modern plate margin suites, most workers now favour an ensialic tectonic setting for the Proterozoic of northern Australia, (Duff & Langworthy, 1974; Stewart et al., 1984; Kroner, 1977; Etheridge et al., in prep).

Detailed mapping and study of the Harts Range Area by staff and students of the University of Adelaide, Department of Geology and Geophysics, has revealed the complexity of its structural evolution. James and Ding (in prep.) consider this area represents "an exhumed classical example of two highly discordant cross-cutting intraplate Early-Mid Proterozoic extension-collision cyclical orogens". These two orogens, the Strangways Orogenic Belt (SOB) and the Harts Range Orogenic Belt (HROB), are considered to be genetically related, the accumulation of the supra- crustal precursors of the HROB associated with extensional faulting of the SOB. The recognition of repeated extensional and contractional tectonic regimes over a remarkably short time span has led James and Ding (in pre) to propose "Caterpillar Tectonics" to be a common (but newly described) style of Proterozoic orogenisis.

The emphasis of this study has been on the Bruna gneiss following the recognition of complex folding and strain variation within this orthogneiss. Field observations and subsequent strain analyses have led to the following conclusions:

1. The 'basement' lithologies of the Entia gneiss complex have undergone at least three phases of repeated, generally isoclinal, recumbent folding events and peak metamorphism prior to intrusion of the Bruna gneiss. The peak (upper amphibolite) metamorphic event produced a pervasive gneissic banding that has been subsequently folded into recumbent or asymmetric folds without any major overprinting fabrics developed. These lithologies are broadly concordant with the foliation of the structurally overlying Granitic gneiss within the study area (however elsewhere they are truncated by this sublithology of the Bruna gneiss)

2. The 'cover' lithologies of the Irindina supracrustal assemblage have been subject to at least one isoclinal folding event prior to the juxtaposition of this meta-pelitic sequence with the 'basement'. Narrow bands of felsic mylonite and incipient c-plane development indicate the ductile shearing associated with emplacement of the Megacrystic gneiss was not confined to the gneiss

but was accomodated within the supracrustal lithologies as well.

3. The Bruna gneiss is subdivided into two lithologies, the structurally lower Granitic gneiss and overlying (much thinner) Megacrystic gneiss. The Megacrystic gneiss, previously described as mylonite derived from the Granitic gneiss, is interpreted as having been intruded independently from the bulk of the Bruna (ie Granitic) gneiss and has experienced a different subsequent strain history.

4. The foliation of the Granitic gneiss is folded by two generations of tight to isoclinal, recumbent folds that are not observed in the Megacrystic gneiss. The Megacrystic gneiss is therefore believed to have intruded post BD2, possibly syn-BD3. Its relatively high biotite and garnet content may indicate some affinity with the meta-peltitic 'cover' sequence, and it has been suggested that shear heating (due to thrusting) has led to localised melting of the Irindina supracrustals to produce the distinctive, thin but persistent Megacrystic gneiss, (J. Foden, Dept. Seminar, 1986).

5. The 'steep zones' or BF3 folds are essentially confined to subarea II, and are best developed in the central part of the Granitic gneiss. These folds, with a variety of styles, have hinge zones that are approximately perpendicular to the direction of movement, that suggests their formation was associated with the ductile juxtaposition of the 'basement' and 'cover'. It is envisaged that small scale,discreet semi-ductile/brittle surfaces developed throughout the gneisses during BD3. These narrow shear zones probably anastomosed throughout the shear zone, and puntuated 'stick-slip' movement along them has allowed folding of the BS2 into inclined, asymmetric, mesosopic folds, (James et al., in prep). Continuing southwards movement of the 'cover' weakly rotated the BF3 hinges into south closing open folds, these BF4 closures are interpreted to represent the earliest stage of the development of sheath folds, (Bell & Etheridge, 1973)

Figures 6.1 and 6.2 describe, in cartoon form, a possible model for the development of the study area. This tectonic synthesis combines ideas form several sources, (James & Ding, in prep.; Shaw et al., 1984; Kroner, 1981; Etheridge et al., in prep).

Figure 6.1: Tectonic evolution of the Harts Range area.

(a) Early-Middle(?) Proterozoic ensialic basin initiated due to crustal thinning above mantle upwelling (Etheridge et al, in prep; Kroner, 1981). Arkosic, pelitic, calcareous and volcanoclastic sediments deposited with intercalated mafic flows and sills. Extensional regime, formation of precursor of the Strangways Orogenic Belt (James and Ding, in press).
(b) Underplating of partially differentiated lower crust melt. Early granitoids emplaced (*eg* possible protoliths of quartzofeldspathic and felsic gneisses?), possibly felsic and mafic precursors of the Inkamulla granitic gneiss, Huckitta Tonalite?.
(c) Cooling of subcrustal lithosphere, possible delamination of the lower crust forcing intracontinental A subduction (Kroner, 1977; Kroner 1981). Lower crustal melting continues with compressional regime to produce ED_2 peak metamorphism (early-syn intrusion of granitic gneisses (Sullivan, 1985; Stewart, 1985)) into the deforming supracrustal pile. James and Ding (in press) suggest plutonism just postdated the metamorphic peak and probably mark the initiation of large scale thrusting. Migmatisation of quartzofeldspathic gneiss, followed by development of aluminosilicate schists. Amphibolites boudinaged within the gneisses. Strangways Orogenic Belt formed.
(d) Initiation of detachment zone, HRDZ at a high angle to the trend of the SOB. (Note that this may be along the previously described lower crustal suture.) Low angle detachment zone, brittle fracture near surface, extending into ductile shear zone at depth (?) allowing rifting and subsidence (upper, northern block) and development of the Harts Range Cover. See James and Ding (in press) for detailed figures and discussion.
(e) Reversal of stress regime, thrusting along HRDZ, ED_4 and ID_1 isoclinal folding due to this deformation? Wide shear zone, mylonites formed under varying metamorphic grades within this wide zone that includes the basement and cover.

Figure 6.1

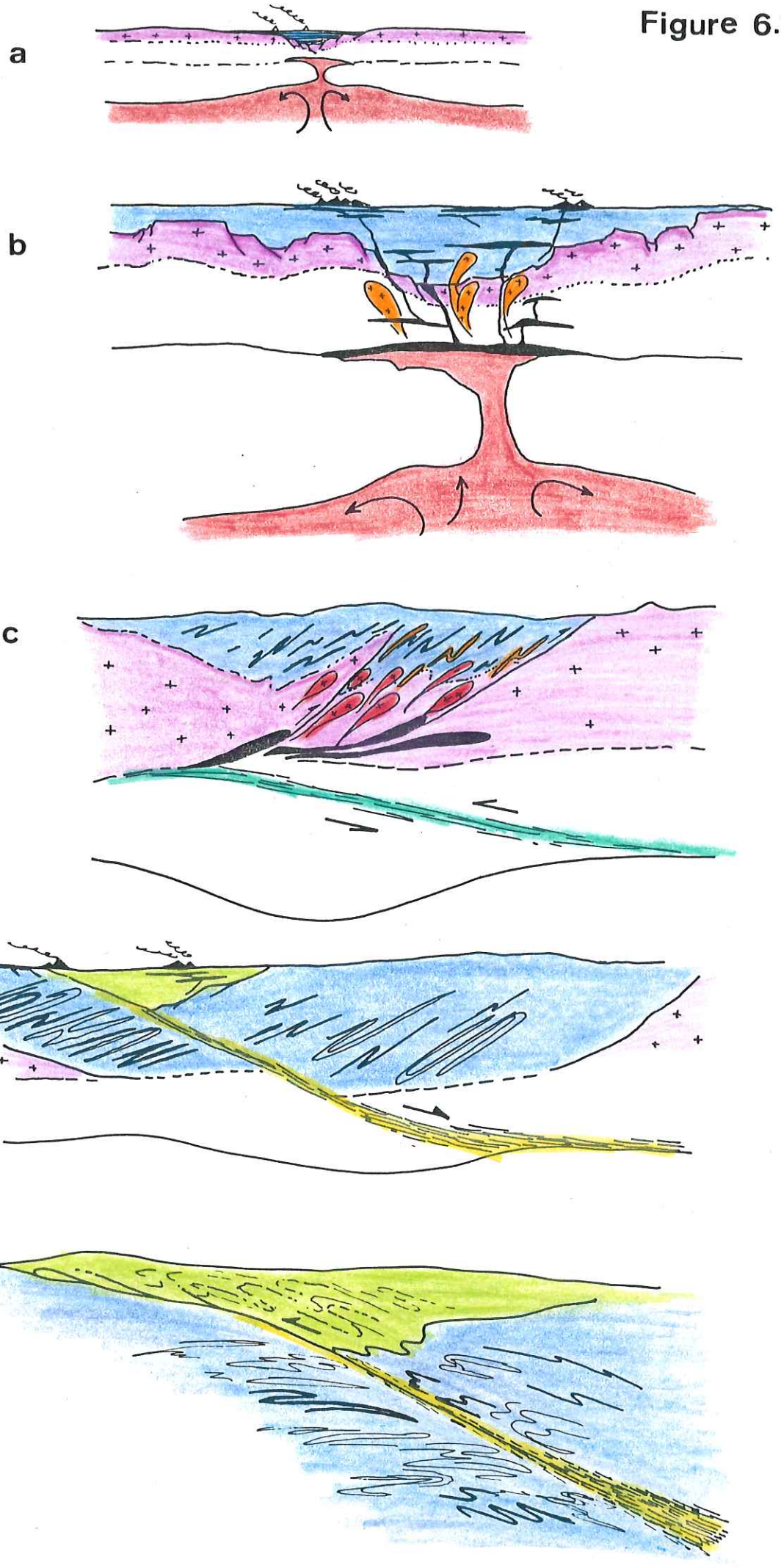

Figure 6.2: Structural development of the Bruna gneiss.

(a) Intrusion of the Granitic gneiss component of the Bruna gneiss incorporating xenoliths of the 'basement'. Early foliation developing whilst still partially molten. The bulk of the movement within the shear zone taken up by the Granitic gneiss but with narrow zones of shear occurring within adjacent lithologies.
(b) Small scale isoclinal recumbent folds produced within the Granitic gneiss by continued shearing within the orthogneiss.
(c) Continuing shearing, concentrated along the upper and lower margins of the Granitic gneiss. Shear heating(?) initiated melting of supracrustal and shear zone lithologies giving rise to the Megacrystic gneiss that intruded along the upper contact. Synchronous isoclinal folding of the Megacrystic/Granitic contact. Small apophyses of the Megacrystic protolith intruded the 'cover'.
(d) Small scale, discreet semiductile/brittle surfaces developed throughout the two gneisses (BD_3). Punctuated 'stick-slip' movement along the surfaces folds the BS_2 into inclined asymmetric folds. Continued southwards movement of the 'cover' weakly rotates BF_3 hinges into southward closing open folds.
(e) Upper contact of the Megacrystic gneiss folded into upright antiformal 'noses' (BF_5).

Figure 6.2

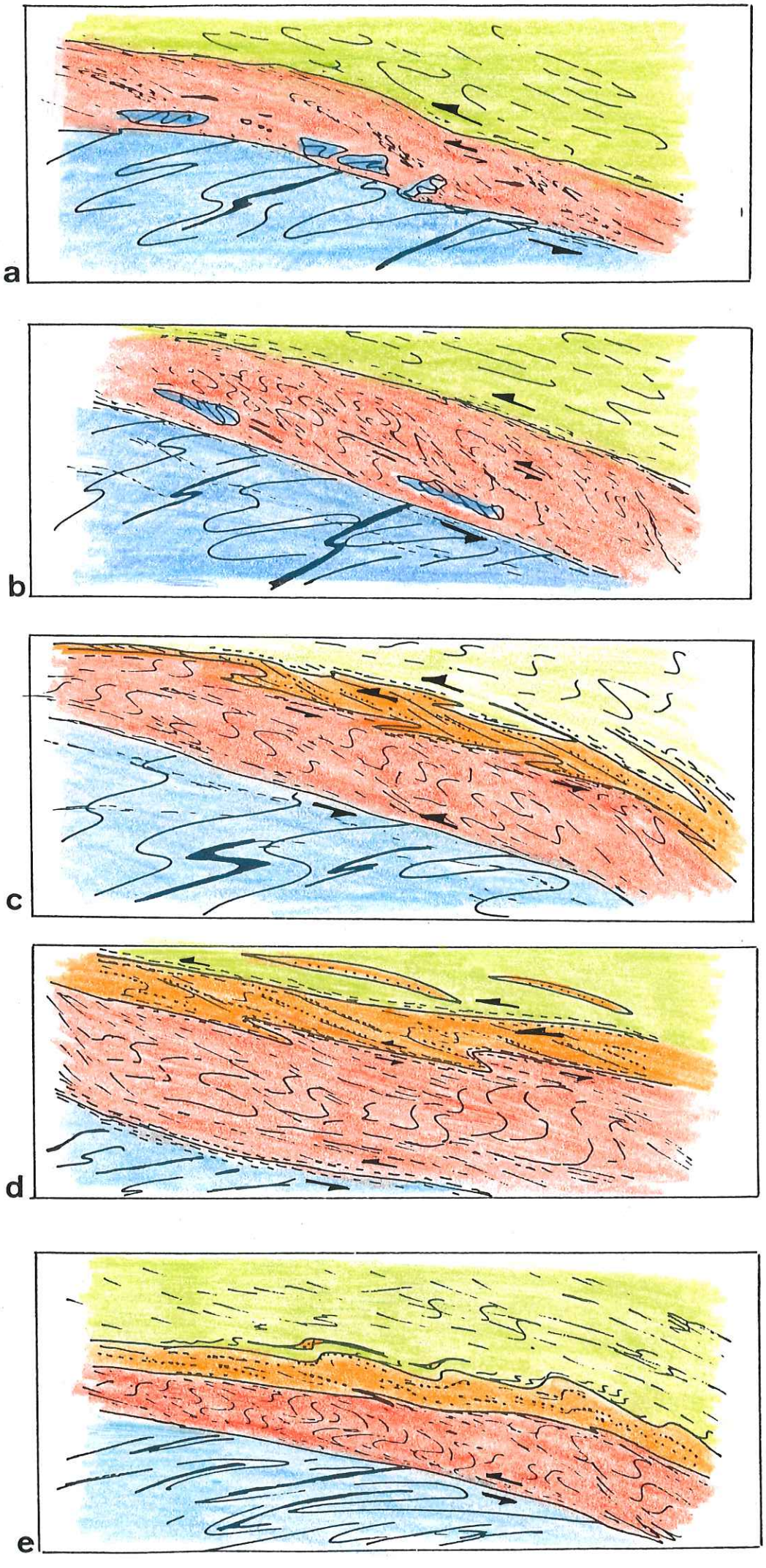

Acknowledgements

Firstly, I wish to thank my supervisor Dr Pat James for his advice, encouragement and patience! throughout the year. Special thanks are also due to Dr John Foden for helpful discussion both in the field and department. I am indebted to Leigh Rankin for his advice, enthusiatic discussion and the loan of many texts and references that have been invaluable. This study has benefited from discussion with Puquan Ding and Rob Lawrence.

This thesis could not have been produced without the assistance of Geoff Trevelyan in thin section preparation, Evert Bleys and Rick Barrett with photography and Sherry Proferes with advice during drafting.

To fellow honours students Meryl and Tony, who shared the fun and frustration of field work in the remote Harts Ranges... thankyou for your unfailing good humour and discussion around the campfire.

To my family, thankyou for your understanding, encouragement (and financial support!) throughout my seemingly endless years at university, and for the eleventh hour polychromatic data enhancement.

To Simon and Peter, with whom I have shared many pizza's, beers and laughs .....cheers!

Most importantly– Alex, thankyou for everything... this thesis is for you.

References

ALM, O., RÖSHOFF, K., AND STEPHANSSON, O., 1980. Microstructures and mechanical characteristics of the Tännäs augen gneiss, Swedish Caledonians. *Geologiska Föreningens i Stockholm Förhandlingar*, 102(4):319–334.

BELL, T. H. AND ETHERIDGE, M. A., 1973. Microstructures of mylonites and their descriptive terminology. *Lithos*, 6:337–348.

BELL, T. H., 1978. Progressive deformation and re-orientation of fold axes in a ductile mylonite zone: the Woodroofe thrust. *Tectonophysics*, 44:285–320.

BERTHE, D., CHOUKROUNE, P., AND JEGOUZO, P., 1979. Orthogneiss, mylonite and non-coaxial deformation of granites: the example of the South Armorican Shear Zone. *J. Structural Geology*, 1:31–42.

BROWN, W. L., MACAUDIÈRE, J., OHNENSTETTER, D., AND OHNENSTETTER, M., 1980. Ductile shear zones in a meta-anorthosite from Harris, Scotland: texural and compositional changes. *J. Structural Geology*, 2(1/2):281–287.

BRUNEL, M., 1986. Ductile thrusting in the Himalayas: shear sense criteria and stretching lineations. *Tectonophysics*, 5(2):247–265.

BUICK, I. S., 1983. The geology, petrology and geochemistry of the Huckitta granodioritic gneiss and associated granitoids, Harts Range, central Australia. Honours Thesis, University of Adelaide. (unpublished)

BURG, J. P., 1986. Quartz shape fabric variations and c-axis fabrics in a ribbon-mylonite: arguments for an oscillating foliation. *J. Structural Geology*, 8(2):123–131.

CULSHAW, N. G. AND FYSON, W. K., 1984. Quartz ribbons in high grade granitic gneiss: modifications of dynamically formed quartz c-axis prefered orientation by oriented grain growth. *J. Structural Geology*, 6(6):663–668.

DING, P. AND JAMES, P. R., 1985. Structural evolution of the Harts Range area and its implications for the development of the Arunta Block, central Australia. *Precambrian Research*, 27:251–276.

DUFF, B. A. AND LANGWORTHY, A. P., 1974. Orogenic zones in central Australia : intraplate tectonics? *Nature*, 249:645–647.

ETHERIDGE, M. A. AND HOBBS, D. E., 1974. Chemical and deformational controls on recrystallisation of mica. *Contr. Mineral. and Petrol.*, 43:111–124.

ETHERIDGE, M. A., RUTLAND, R. W. R., AND WYBORN, L. A. I., IN PREP. Orogenesis and tectonic processes in the Early to Middle Proterozoic of Northern Australia. in prep.

EVANS, D. J. AND WHITE, S. H., 1984. Microstructural and fabric studies from the rocks of the Moine Nappe, Eriboll, N. W. Scotland. *J. Structural Geology*, 6:369–389.

FODEN, J. D. AND BUICK, I. S., 1986. Petrology, geochemistry and crustal development, Entia Dome, Eastern Arunta Block, Northern Territory. In *Abstract Eigth Aust. Geol. Conv.*, Adelaide.

FODEN, J. D., 1980. The geology of the Entia Domal Structure, eastern Harts Ranges, N. T. In Shaw, R. D., Warren, R. G., Glikson, A. Y., James, P. R., Lawrence, R. W., Oliver, R. L., and Foden, J. D., editors, *Excursion Guide-Arunta Block*, Bur. Min. Res. Geol. Geophys. Record :27.

GAPAIS, D. AND BARBARIN, B., 1986. quartz fabric transition in a cooling syntectonic granite (Hermitige Massif, France). *Tectonophysics*, 124:357–370.

GOSCOMBE, B., 1984. The Structure, Metamorphism, Petrology and Geochemistry of the Paradise Well Area in the Harts Ranges, Eastern Arunta Block. Honours Thesis, University of Adelaide. (unpublished)

HOBBS, B. E., MEANS, W. D., AND WILLIAMS, P. F., 1976. *An Outline of Structural Geology*. Wiley, New York, NY.

JAMES, P. R. AND DING, P., in press. "Caterpillar Tectonics" in the Harts Range area: a kinship between two sequential Protozoic extension-collision orogenic belts within the Eastern Arunta Inlier of central Australia.

JAMES, P. R., DING, P., RANKIN, L., AND SCALES, G., 1985. Displacement and strain within the nappe sequences of the Harts Range area, central Australia. In *Abstracts vol. of IGCP conference: Tectonics and geochemistry of Early to Middle Proterozoic Fold Belts*, Darwin, August.

JAMES, P. R., MACDONALD, P., AND PARKER, M., IN PREP. Strain and displacement in the Harts Range detachment zone: a study of the Bruna Gneiss and its bounding faults from the eastern margin of the Entia Dome, central Australia. in prep.

JOKLIK, G. F., 1955. The Geology and mica fields of the Harts Range, central Australia. *Aust. Bur. Min. Res., Geol. Geophys. Bull.*, 26.

KRONER, A., 1977. Precambrian mobile belts of southern and eastern Africa-Ancient sutures or sites of ensialic mobility? *Tectonophysics*, 40:101–135.

KRONER, A., 1981. *Precambrian Plate Tectonics*. Elsevier.

LAW, R. D., KNIPEW, R. J., AND DAYAN, H., 1984. Strain thrust within thrust sheets; microstructural and petrofabric evidence from the Moine Thrust zone at Loch Eriboll, Northwest Scotland. *J. Structural Geology*, 6(5):477–497.

LAWRENCE, R. W., in prep. *The structure and metamorphism of the Irindina supracrustal assemblage on the western side of the Entia Dome, Harts Range, central Australia.* PhD thesis, University of Adelaide. (unpublished)

MARTIN, A., 1983. The Geology and Structural Geology of the Harts Range Group on the East Flank of the Etia Dome, Eastern Arunta Block. Honours Thesis, University of Adelaide. (unpublished)

MYERS, J. S., 1984. *The Nagssugtoqidian mobile belt of Greenland*, pages 237–250. E. Schweizerbartsche Verlagsbuchhandlung.

OBEE, H. K. AND WHITE, S. H., 1985. Faults and associated fault rocks of the southern Arunta Block, Alice Springs, Central Australia. *J. Structural Geology*, 7/6:701–712.

OLIVER, R. L. AND FODEN, J. D., 1986. Metamorphism and melting in the Eastern Harts Ranges, N. T. In *Abstracts of SGGMP Papers at 8th Aust. Geol. Conv.*, Adelaide.

PARKER, M. D., in prep. A structural and lithological investigation of the southern Mt Bruna area, with special reference to the Bruna Gneiss, western Entia Dome, Harts Range, central Australia. Honours thesis, University of Adelaide. (unpublished)

PLUMB, K. A., DERRICK, G. M., NEEDHAM, R. S., AND SHAW, R. D., 1981. Precambrian of the southern hemisphere. In Hunter, D. R., editor, *Precambrian of the Southern Hemisphere : Developments in Precambrian Geology, Volume 2*, pages 205–307, Elsevier.

RAMSAY, J. G. AND HUBER, M. I., 1983. *The Techniques of Modern Structural Geology.* Volume 1, Academic Press.

RAMSAY, J. G., 1967. *Folding and fracturing of rocks.* McGraw-Hill, New York.

RANKIN, L. R. AND JAMES, P. R., 1984. The development of high grade tectonothermal fabrics and mylonites associated with complex ductile deformations in metamorphic basement and cover rocks from Harts Range, central Australia. In *Bermagui'84: international conference on multiple deformation and foliation development.*

RANKIN, L. R., 1983. The Structural Geology and Fabric Development in the Mt. Mabel area of the Harts Range, Eastern Arunta Block. Honours Thesis, University of Adelaide. (unpublished)

SHAW, R. D. AND FREEMAN, M. J., 1985. *Explanatory Notes on the Illogwa Creek Geological Sheet (2nd Edition).* Technical Report, Bur. Min. Res.

SHAW, R. D. AND STEWART, A. J., 1975. Towards a stratigraphy of the Arunta Block. In *Abstracts of the 1st. Geol. Soc. Aust. Conv.*

SHAW, R. D., FREEMAN, M. J., OFFE, L. A., AND SENIOR, B. R., 1982. Geology of the Illogwa Creek, 1:250 000 sheet area, central Australia — Preliminary Data 1979–80 surveys. *Bur. Min Res Geol Geophys Record.*

SHAW, R. D., STEWART, A. J., AND BLACK, L. P., 1984. The Arunta Inlier: a complex ensialic mobile belt in central Australia, Part 1. *Aust. J. Earth Sci.*, 31:457–484.

SIBSON, R. H., 1977. Fault rocks and fault mechanisms. *J. Geol. Soc. London*, 133:191–213.

SILLS, J. D. AND TARNEY, J., 1984. Petrogenesis and tectonic significance of amphibolites interlayered with meta-sedimentary gneiss in the Ivrea Zone, southern Alps, Northwest Italy. *Tectonophysics*, 107:187–206.

SIMPSON, C. AND SCHMID, S. M., 1983. An evaluation of the criteria to deduce the sense of movement in sheared rocks. *Bull. Geol. Soc. Am.*, 94:1281–1288.

SIVELL, W. J. AND FODEN, J. D., 1985. Banded amphibolites of the Harts Range meta-igneous complex, central Australia; a bimodal basalt-tonalite suite. *Precambrian Research*, 28:223–253.

SODRE BORGES, F. AND WHITE, S. H., 1980. Microstructural and chemical studies of sheared anorthosites, Roneval, South Harris. *J. Structural Geology*, 2(1/2):273–280.

STEWART, K. P., 1985. The petrological significance of calc-silicates and associated gneisses, Inkamulla well area, N. T. Honours Thesis, University of Adelaide. (unpublished)

STEWART, A. J., SHAW, R. D., AND BLACK, L. P., 1984. The Arunta Inlier: a complex ensialic mobile belt in central Australia, Part 2. *Aust. J. Earth Sci.*, 31:445–455.

SULLIVAN, S. J., 1985. A detailed geological investigation of the Entia Gneiss and Leucocratic Gneiss intrusive, Nthrn. Entia Dome, Harts Range, Eastern Arunta Block. Honours Thesis, University of Adelaide. (unpublished)

TAKAGI, H., 1986. Implications of mylonitic microstructures for the geotectonic evolution of the Median Tectonic Line, Central Japan. *J. Structural Geology*, 8(1):3–14.

TEYSIER, C., 1985. A crustal thrust system in an intracratonic tectonic environment. *J. Structural Geology*, 7/6:689–700.

TURNER, F. J. AND WEISS, L. E., 1963. *Structural Analysis of Metamorphic Tectonites*. McGraw-Hill, New York, NY.

VERNON, R. H., 1986. K-feldspar megacrysts in granites – Phenocrysts not porphyroblasts. *Earth Science Reviews*, 23:1–63.

WATTS, M. J. AND WILLIAMS, G. D., 1983. Strain geometry, microstructure and mineral chemistry in metagabbro shear zones: a study of softening mechanisms during progressive mylonization. *J. Structural Geology*, 5(5):507–517.

WHITE, S., 1976. The effects of strain on the microstructures, fabrics, and the deformation mechanisms in quartzites. *Phil. Trans. R. Soc. Lond. A.*, 283:69–86.

WHITE, S. H., 1982. Fault rocks of the Moine Thrust Zone; a guide to their nomenclature. *Textures and Microstructures.*, 4:211–221.

WHITE, S. H., BURROWS, S. E., CARRERAS, J., SHAW, N. D., AND HUMPHREYS, F. J., 1980. On mylonites in ductile shear zones. *J. Structural Geology*, 2:175–188.

LAWRENCE, R.W., JAMES, P.R. AND OLIVER, R.L. (IN PREP.) Relative timing of folding and metamorphism in the ruby mine area of the Harts Range, central Australia.

SAMPLE LOCALITY MAP

ALL SAMPLES ARE PREFIXED BY 865/-

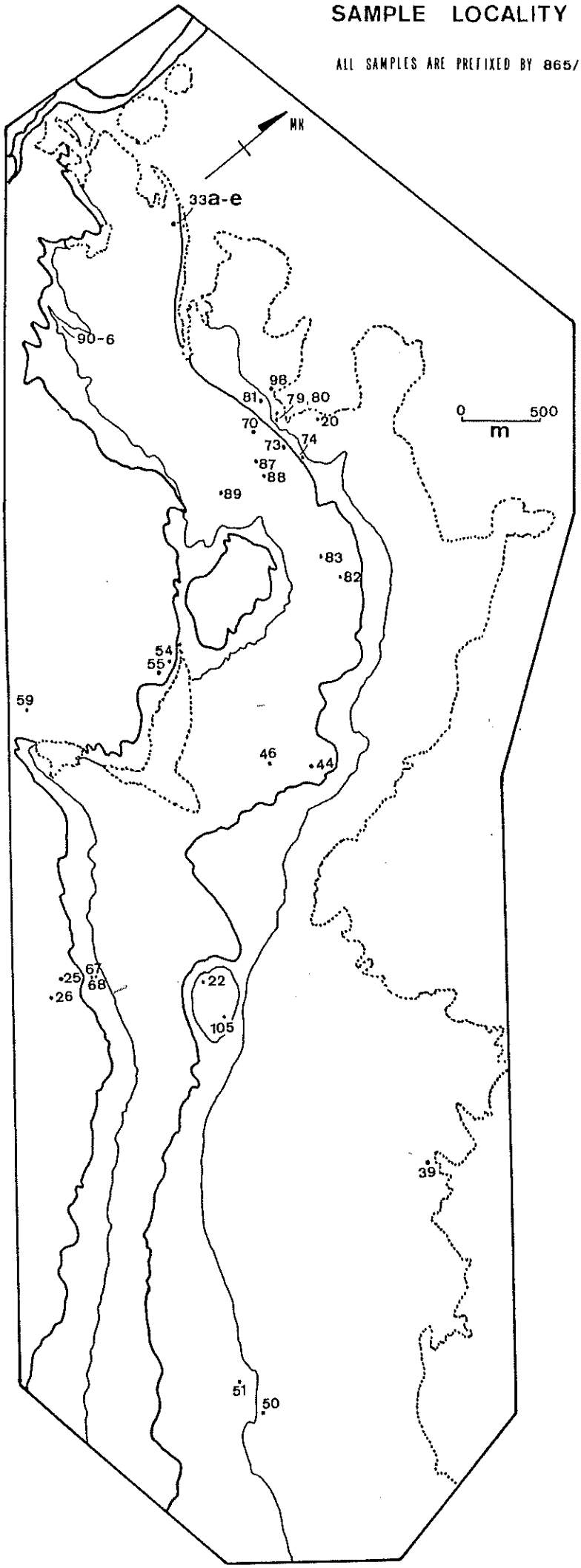

Appendix I
Thin Section Descriptions

Locations of samples described throughout this study are shown in the sample locality map in this appendix. Thin section preparation is described in Appendix II.

Granitic gneiss — 865–44

Hand Specimen:
A cream to orange finely layered, faintly lineated, fine grained granoblastic gneiss.

Thin Section:
A remarkably even grained granoblastic polygonal gneiss with the fabric weakly defined by quartz ribbons (0.3mm) and scattered aligned pale-green to black biotite laths. Some grains show a shape-preferred orientation but overall the feldspathic grains are of a homogeneous equant grainsize and shape.

- K-feldspar 40%: Granoblastic equant to elongate medium grain size, strongly developed strain shadowing and diffuse cross-hatched twinning. Recrystallising to fine grained aggregates along grain boundary margins.
- Quartz 25%: Very difficult to distinguish from untwinned feldspar. It has no alteration but is pitted and contains numerous very fine inclusions. Usually forming ribbons of elongate grains with boundaries perpendicular to its length. Strain shadowing common.
- Plagioclase 30%: Preferentially sericitised (relative to microcline) and generally more so around rims and along twin planes. Some have K-feldspar or quartz cores recrystallised. Plagioclase rarely occurs with thin rims of K-feldspar.
- Biotite 5–15%: Single grains, ragged altered to reddish nonpleochroic material parallel to (001). Pleochroic pale yellow green to dark brown.
- Muscovite 5%: Coarse, ragged, white muscovite inter-grown with K-feldspar along plagioclase grain margins.

Elongate quartz grains, single biotite laths and medium grained euhedral to anhedral opaques define the foliation.

Granitic gneiss — 865–96

Hand Specimen:
A medium grained streaky grey gneiss with small clots of hornblende visible.

Thin Section:
A medium to fine grained augen feldspathic gneiss with augen (2–7mm in diameter) consisting of plagioclase aggregates that include small (0.01mm) irregular to rounded biotite and hornblende within the grains and randomly oriented along feldspar margins. Quartz ribbons observed only in the XZ section. Distinct elongate granoblastic feldspathic matrix contains spaced, anastomosing aggregates of biotite that include elongate hornblende, garnet and opaques.

- K-feldspar 30%: Coarse grained augen of microcline/microperthite are partially recrystallised to fine grained granoblastic margins.
- Plagioclase 30%: Moderately polysynthetically plagioclase megacrysts with fewer inclusions of biotite than observed in the K-feldspar.
- Quartz 20%: Medium irregular grains granoblastic elongate with strong deformation banding.
- Biotite 20%: Large (1mm) laths occur in decussate aggregates. Pleochroic straw yellow to khaki green, appear to be associated with skeletal garnet.
- Garnet 5%: Strongly embayed elongate, fractured(?) garnets contain numerous inclusions of subrounded quartz, and biotite, hornblende, epidote(?) and apatite(?).

Accessory minerals include fine grained epidote as rims around opaques, fine grains of yellow/gold-brown, faintly pleochroic allanite, pale yellow to deep blue green hornblende and fine egg shaped grains of apatite.

Megacrystic gneiss — 865–67

Hand Specimen:
A medium to fine grained pink and grey well layered gneiss weathering to a dark chocolate brown schistose rock. The feldspar megacrysts in this sample appear strongly flattened to produce attenuated ribbons.

Thin Section:

- Plagioclase 32%: Porphyroblasts being altered around the margins to new finer untwinned grains. Some large grains show slight bending of the albite twins and tapering pericline twinning is common. Some grains strongly

sericitized. Curved, to straight oriented weakly lobbed margins between plagioclase grains. AB62 to AB55 determined via Michel-Levy Method. Coarse grained, elongate plagioclase megacrysts are wrapped by a well developed preferred orientation foliation defined by biotite and quartz grains.

- K-feldspar 25%: Fine grained equigranular to ineqigranular, polygonal to interlobate of variable grain size. Grains commonly rounded oriented lobbed with wide diffuse boundaries. Patchy extinction very common with diffuse twinning.
- Quartz 20%: Form thick ribbons up to 1mm wide in relatively biotite-poor layers. Composed of rectangular unstrained segments with curved quartz quartz boundaries. Lobbate against matrix grains.
- Biotite 15%: Medium to fine grained, pleochroic golden/straw yellow to deep brown elongate with diffuse ragged ends, less commonly embayed along the lengths. Coarser grains occur in aggregates parallel to the compositional banding, finer ragged grains occur perpendicular to fabric. Strongly associated with hornblende, apparently replacing it along the amphibole cleavages.
- Garnet 3%: 0.25mm to 1mm large strongly altered elongate. Moderately fractured, commonly at a high angle to the fabric with replacement by quartz initiated along them. Marginal inclusions of opaques, biotite, and K-feldspar(?). Very pale brown and non-pleochroic.

Accessories include opaques, amphibole, zircon and apatite. In the XZ section opaques are more elongate, porphyroblasts are strongly sericitized and feldspars have more distinct undulose extinction, twins more strongly deformed. Biotite stacks define low-angle inclined surfaces.

Megacrystic Bruna — 865–68

Hand Specimen:
Very coarse grained augen-bearing schistose gneiss with cream and pink feldspar megacrysts, subrounded to extremely elongate up to 5cm diameter.

Thin Section:
A well foliate inequigranular megacrystic quartz feldspar biotite gneiss with extremely large subrounded to elongate megacrysts of partially to completely recrystallised feldspar quartz garnet and hornblende set in an equigranular polygonal to elongate granoblastic fine grained matrix. The fabric is defined by brownish green to pale blue lepidoblastic biotite.

- Feldspar 20–30%: Large K-feldspar porphyroblasts are generally highly strained with patchy undulose extinction and advanced subgrain development. Very similar to quartz however numerous *en echelon* inclusions, faint

cryptoperthitic texture and biaxial positive figure indicate K-feldspar. General shape is subrounded with margins finely embayed or serate with few straight boundaries. 'mortar texture' is common and there is invariably a rind of very fine grained matrix between porphyroblasts and biotite oriented quartz streaks. Subrounded to elongate zones of myrmekite near margins.

- Plagioclase 20–35%: Generally smaller porphyroblasts of well twinned (polysynthetic albite and pericline). Several megacrysts contain biotite at their core often oriented at a high angle to the external fabric. Pericline twins, often bent several examples of infilled fractures.

- Biotite 10–30%: Strongly pleochroic, pale brown to dark brown biotite as single idioblastic laths or decussate strings. Appears to be 2 generations of biotite, one the coarse grained aggregates and two, fine grained equant isolated laths pinning quartz and feldspar grain boundaries.

Other minerals include pale-green to deep green anhedral hornblende, very pale cream attenuated garnet and subidioblastic equant epidote usually associated with biotite around garnets.

Entia Megacrystic Chlorite Schist — 865–20

Hand Specimen:
White pebble-sized feldspar augen (up to 15mm inequigranular diameter) set in a fine grained pale-green chlorite schist.

Thin Section:

- Plagioclase 30–60%: Occurs as very large rounded megacrysts with thin widely spaced albite twins. Mildly sericitized around margins and along fractures. Subgrain development visible close to its margins. Plagioclase also occurs in the matrix as strongly sericitized (polysynthetic twinned) elongate aggregates.

- Chlorite 30 %: Nematoblastic sheaths of pleochroic pale to medium green chlorite anastomose around the elongate aggregates of plagioclase or mosaic quartz. Becomes very coarse grained in pressure shadows adjacent to larger plagioclase augen.

- Quartz 30%: Medium to fine grain extremely elongate grains serate to lobate highly strained close to margins.

Scattered skeletal to subhedral epidote, colourless non-pleochroic twinned with cores of low relief colourless material. Ragged deep green hornblende grains rare.

Entia Meta-ultramafic Pod — 865–22

Hand Specimen:
A variety of lithologies appear within this subcircular outcrop including olivine bearing metaperidotite, hornblendite and amphibolite. The hand specimens vary from massive, heavy, black, medium grained samples to strongly weathered schistose samples.

Thin Section:
The metaperidotite consists of large (2–6mm), poikilitic and skeletal clinopyroxene that includes highly fractured anhedral olivine set within a very fine grained recrystallised matrix that possibly consists of finely intergrown clinopyroxene and plagioclase.

- Clinopyroxene (augite?) 25%: Very pale green, non-pleochroic finely striated skeletal grains. Strongly altered to faintly brown mush. Low birefringence (upper first order), showing anomalous blue or green close to extinction.
- Olivine 15%: Small (less than 0.5mm) subrounded to ragged, highly fractured colourless to yellow-brown. Moderately high relief with thick, dark, grain boundaries.
- Plagioclase 10%: Coarse grained (up to 3mm) strongly embayed irregular grains. Fine polysynthetic twinning pseudomorphed internally and externally by matrix.

The matrix (up to 60%) is non-pleochroic and faintly green, pseudomorphing all major mineral phases. Accessory phases include spinel, probably chromite as high relief, rounded, spotted, isotropic grains. Some pleonaste may be present (very fine blebs of isotropic/leafy-green). Weakly pleochroic pale-yellow to pale-gold mica is associated with some opaques.

Entia Massive Amphibolite — 865–50

Hand Specimen:
Dark grey, weathered, coarse grained amphibolite with pale augen of plagioclase. A very faint foliation due to nematoblastic hornblende is visible.

Thin Section:
Coarse grained granoblastic inequigranular hornblende, plagioclase amphibolite.

- Hornblende 60%: Pale to deep green pleochroic anhedral grains up to 5mm long, simple twinned, embayed. Numerous rounded to elongate colourless to faintly green diopside(?) grains lie along cleavages. Secondary hornblende preferentially recrystallising at the vertices of the hornblende prisms.

- Plagioclase 30%: Frequent aggregates of strongly sericitized augen. Strongly deformed with curved polysynthetic twins and fractured pericline and albite twins. Grain margins tend to be irregular to lobate. Finer grained unstrained (*ie* untwinned) polygonal grains occur within the hornblende rich layer and between secondary hornblende and remnant clinopyroxene. These grains contain rare simple twins and inequiangular triple-point junctions.

- Quartz 5%: Uncommon, large (greater than 2mm), anhedral grains with a cloudy appearance and strong deformation banding. Occur in small attenuated segregations.

Strongly altered skeletal augite(?) rarely occurs as finely striated brown patches.

Entia Felsic gneiss — 865–33f

Hand Specimen:
A pale, orange-brown, well foliated augen gneiss with pink perthitic microcline megacrysts 3–15mm in diameter and large (2mm) hornblende grains. Elongate K-feldspar streaks and hornblende aggregates parallel the composition banding.

Thin Section:
A very coarse to fine grained (*ie* bimodal) feldspathic granoblastic elongate gneiss.

- K-feldspar 40%: Perthitic and microperthitic K-feldspar megacrysts show faint strain shadowing and weak mortar texture around the margins. Sinuous exsolution streaks trend inwards from the margins and myrmekite patches occur close to the megacryst margins in the matrix.

- Plagioclase 20%: Strongly sericitized with intense strain shadowing and grain margins bulging outward into adjacent quartz grains. Vermicular intergrowths with quartz are common. Very fine granular material and yellow staining occurs along feldspar contacts. Numerous clear subrounded inclusions.

- Quartz 20%: Quartz grains relatively more elongate with intense deformation banding perpendicular to their length.

Other mineral phases include pale green to blue green irregular hornblendes, minor biotite, pale pink garnet and sphene.

Strongly altered skeletal augite(?) rarely occurs as finely striated brown patches.

Entia Calc-silicate — 865–80

Hand Specimen:
The mafic calc-silicates are finely banded pink to dark green, with small irregular coarsely crystalline, hornblende rich streaks and boudins.

Thin Section:
Medium to fine grained granoblastic polygonal to elongate (essentially monomineralic) laminae of hornblende, epidote, scapolite, plagioclase, quartz, clinopyroxene, minor diopside, sphene and zircon.

- Hornblende (up to 50%): Coarse grained anhedral elongate simple twinned brown to green moderately recrystallised. Defines a strong L-S fabric.
- Plagioclase (up to 30%): Granoblastic with smooth curving margins, triple-point junctions and small new egg-shaped grains along grain margins.
- Quartz (up to 45%): Defining extremely regular thin (less than 1mm) straight margined sheets composed of tabular subgrains and grains. Deformation banding perpendicular or at 45° to the ribbons. Note similar optical orientation of the longer grains.
- Epidote (up to 80%): Very pale green non-pleochroic elongate grains with gently curving margins. Zoning of pale yellow birefringence distinctive.
- Scapolite (up to 30%): Uniaxial negative, steel grey to blue anomalous birefringence. Grains tend to be tabular with one cleavage visible.

Large (greater than 4mm) elongate brownish patches of clinopyroxene(?) contain numerous very small rounded inclusions of epidote(?) and quartz.

Irindina Amphibolite — 865–25

Hand Specimen:
A fine grained dark grey massive mafic, fabric not visible in hand specimen.

Thin Section:
A fine grained, well foliated hornblendite/amphibolite.

- Hornblende 60%: Faint bluish-green to olive-green subhedral to anhedral elongate aggregates and prisms with gently curved to lobed grain boundaries. Occasional twin planes parallel to the nematoblastic fabric.
- Plagioclase (up to 30%): Evenly distributed irregularly shaped aggregates of polygonal grains with triple-point junctions and straight grain boundaries. Rare albite twins visible. Grains become elongate in hornblende poor zones.

- Opaques 10%: Equant fine grained rounded to square but sometimes skeletal with transparent reddish margins. Commonly occurring along hornblende margins but also contained within the hornblende and rarely at plagioclase junctions. Evenly scattered throughout.

Small microfaults infrequently displace hornblende cleavages and the hornblende appears to be recrystallising to paler green fine grained aggregates.

Appendix II
Thin Section Preparation

1. Thin sections of both the XZ and YZ sections of the specimen were prepared, with the orientations of X, Y and Z recorded on each section. (After Turner & Weiss, 1963.)

2. The section is stained to differentiate quartz grains (colourless) from plagioclase (red) and alkali feldspar (yellow) using the following technique:

   (a) Etch the section for 60 seconds in hydroflouric acid vapour.

   (b) Immerse in a saturated solution of sodium cobaltinitrite for 15 seconds.

   (c) Rinse briefly in tap water.

   (d) Immerse for 5 seconds in a solution of barium chloride.

   (e) Dip in distilled water.

   (f) Immerse for 60 seconds in a solution of amaranth.

   (g) Dry section with a gentle stream of compressed air.

It was noted that the yellow stain for K-feldspar (sodium cobaltinitrite) deteriorated with subsequent immersion in the solution of amaranth. It is suggested that samples only be stained for plagioclase identification as it was found that *etching* was sufficient to clearly highlight K-feldspar cleavages.

Appendix III
Strain Analysis and Methods

Structural Nomenclature

Foliations, folds and lineations are denoted by S_n, F_n and L_n respectively, with the deformation interpreted as responsible for the development being D_n. The subscript n refers to the relative timing of each deformation with the earliest identifiable being D_1. No original sedimentary/igneous layering has been identified in the study area, and so the subscript '0' is not applicable.

Fold Classification Scheme

The scheme of Ramsay (1967) is used in classification of fold types.

Dip Isogon Strain Analysis

In conditions of ductile deformation, it is common for the shape of buckled layers to become modified by the superposition of fairly homogeneous strain. De Sitter suggested that further compressive strain leads to modification of the parallel buckled layers by a process of flattening producing "flattened parallel folds". This modification of an originally parallel fold will produce a fold profile with weakly convergent dip isogons (class 1c) (ie they approach the class 2 similar folds). It is possible, using the graphical methods of Hudleston (1973), to estimate the total compression strain that has acted on the layer. The major assumption is that we must ensure that the original shape was that of a parallel fold.

Experimental Procedure

The % shortening within flattened parallel folds (class 1c) was calculated graphically by separation of the component of layer buckle and the component of homogeneous flattening.

1. Dip isogons are plotted on type 1c fold profiles and a graph of α vs. $(\alpha - \phi)$ plotted (figures IIIa & IIIb). The slope of the line thus drawn is equivalent to $\sqrt{\lambda_2}/\sqrt{\lambda_1}$.

2. A distorted grid with distorted unit axes of $\sqrt{\lambda_1}$ and $\sqrt{\lambda_2}$ is drawn, maintaining unit area to maintain plain strain conditions.

   The extension of the $\sqrt{\lambda_1}$ axis = $\sqrt{\lambda_1'}$

The extension of the $\sqrt{\lambda_2}$ axis $= \sqrt{\lambda_2'}$

(See figure IIIc.)

3. The fold profile is superimposed upon the distorted grid and redrawn to produce an undistorted grid with unit length axes, removing the component of homogeneous flattening from the fold (figure IIId).

4. The buckle component of shortening (B) is calculated by:

$$B = \frac{l_0 - l_1}{l_0} \times 100\%$$

The homogeneous flattening component of shortening (H) is calculated by:

$$H = (100 - B)(1 - \sqrt{\lambda_2'})\%$$

The total % shortening T is then:

$$T = (H + B)\%$$

— From Rankin (1983) after Hudlestone (1973).

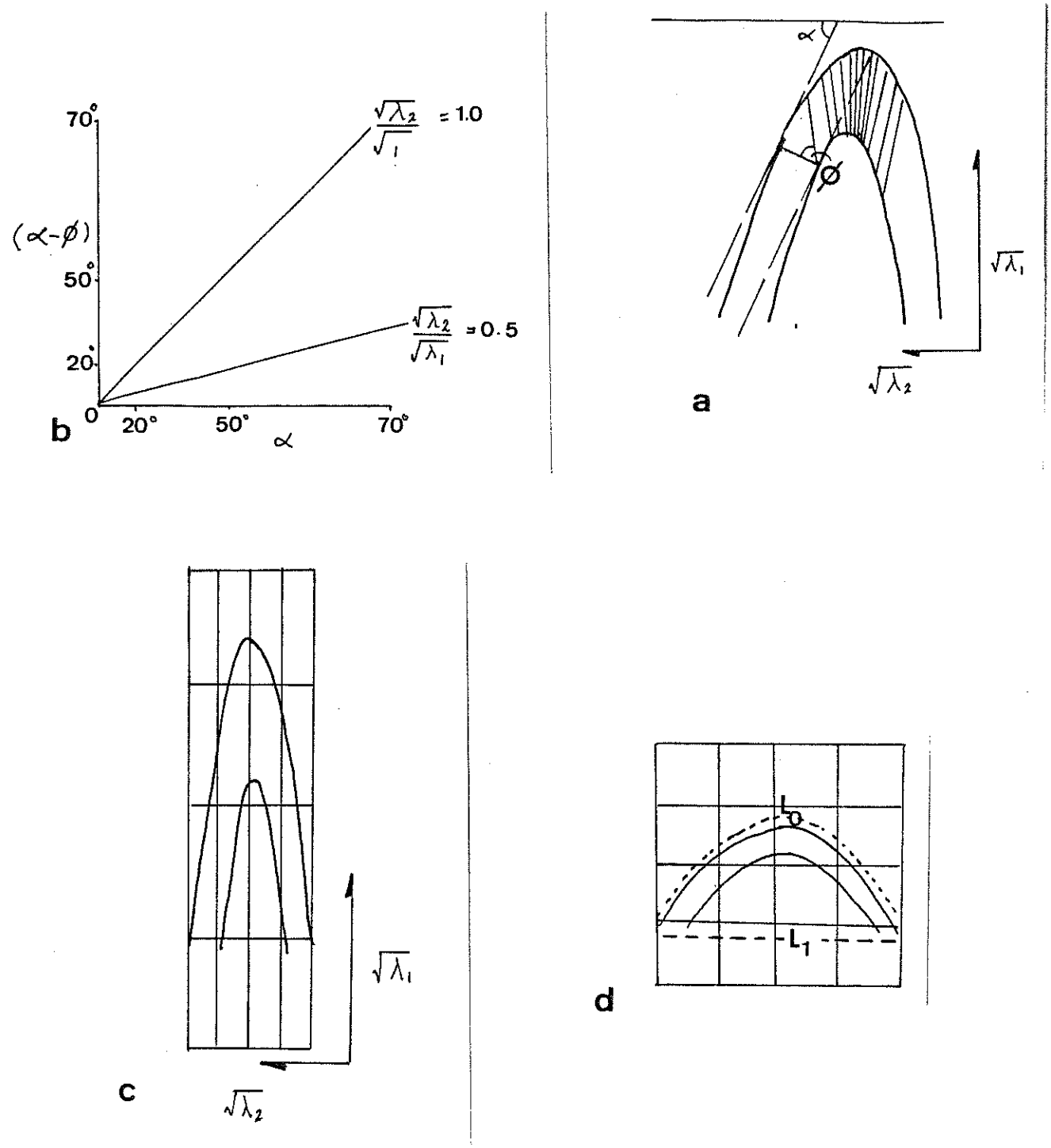

Figure III:

(a) Fold profile of a class 1c fold, showing the relationship of ϕ to the dipisogon for the angle α.

(b) Empirical graph of $(\alpha - \phi)$ vs α. The slope of a straight line $= \sqrt{\lambda_2}/\sqrt{\lambda_1}$.

(c) Distorted grid with superimposed class 1c fold profile.

(d) Undistorted grid with fold profile displaying pre-flattening buckle strain: $l_0 - l_1/l_0$.

THE GEOLOGY OF THE WESTERN MARGIN OF THE ENTIA DOME, HARTS RANGE, N.T.

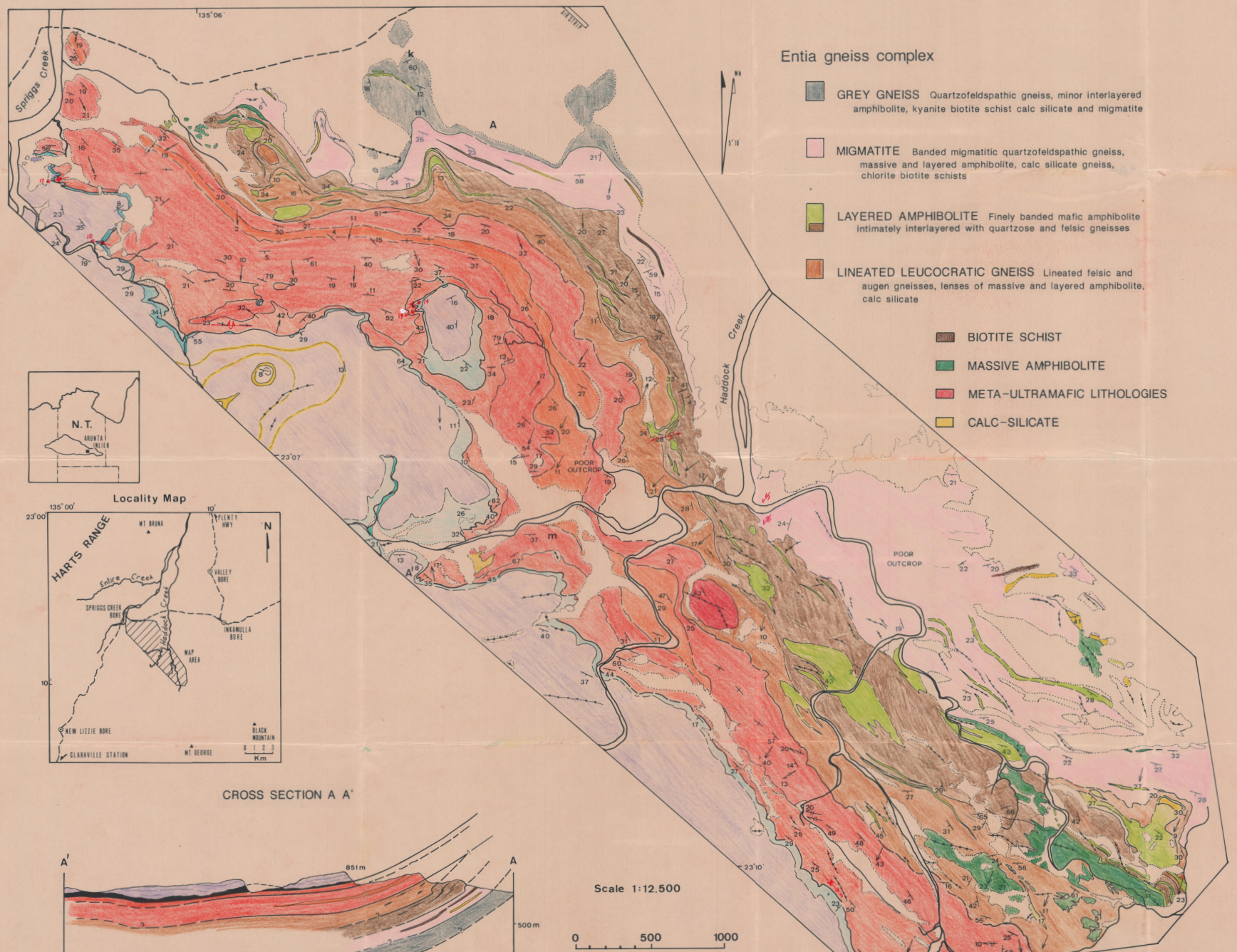

Entia gneiss complex

- GREY GNEISS Quartzofeldspathic gneiss, minor interlayered amphibolite, kyanite biotite schist calc silicate and migmatite
- MIGMATITE Banded migmatitic quartzofeldspathic gneiss, massive and layered amphibolite, calc silicate gneiss, chlorite biotite schists
- LAYERED AMPHIBOLITE Finely banded mafic amphibolite intimately interlayered with quartzose and felsic gneisses
- LINEATED LEUCOCRATIC GNEISS Lineated felsic and augen gneisses, lenses of massive and layered amphibolite, calc silicate
- BIOTITE SCHIST
- MASSIVE AMPHIBOLITE
- META-ULTRAMAFIC LITHOLOGIES
- CALC-SILICATE

Bruna gneiss

- MEGACRYSTIC GNEISS
- GRANITIC GNEISS megacrystic

Irindina supracrustal assemblage

- BIOTITE GARNET SCHIST
- MARBLE calc-silicate
- AMPHIBOLITE

Locality Map

CROSS SECTION A A'

Scale 1:12,500

0 500 1000

- Lithological boundary observed / inferred
- Outcrop boundary
- Foliation inclined / vertical
- structure form lines
- Lineation plunge
- Fold axis upright antiform synform
- overturned antiform synform
- asymmetric with vergence
- minor recumbent
- Pegmatite
- Mineral occurrence kyanite k; mica m; tourmaline t
- Vehicle track
- Watercourse (annual)